Jitter Analysis Techniques for High Data Rates

Application Note 1432

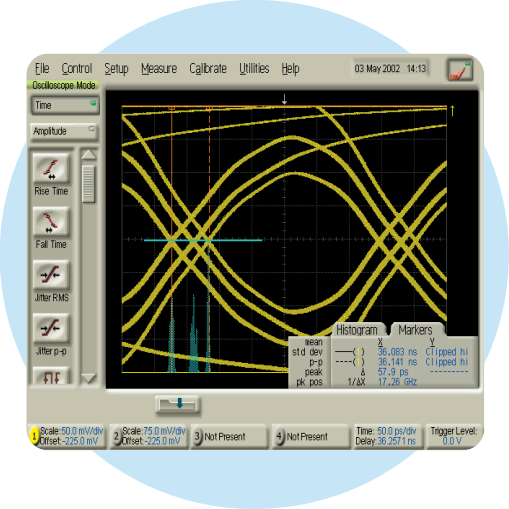

Agilent Technologies

Table of Contents

List of Figures

List of Tables

1. Introduction

The ability to understand, identify and solve serious jitter problems is imperative as data rates exceed the Gb/s level. From SONet/SDH networks at OC 768—nearly 40 Gb/s—to Gigabit Ethernet and 10 Gigabit Ethernet, low data rate jitter analysis techniques that use real-time data acquisition such as Time Interval Analysis (TIA)[1], cycle-to-cycle, and period jitter analysis[2] are less useful. At high data rates techniques like low noise phase detection, high speed sampling, and indirect analysis methods are necessary.

To fix difficult jitter problems, engineers need to understand the diverse techniques used in both synchronous and asynchronous networking. This note gives a concise presentation of jitter theory with descriptions of the common techniques used by SONet/SDH, Gigabit Ethernet and Fibre Channel engineers to understand the jitter performance of high data rate networking components and systems. Descriptions of how the techniques are implemented on Agilent Technologies' equipment illustrate the theory and help engineers decide on the best solution for their job.

The techniques described here cover jitter analysis applications across the spectrum from research and development through diagnostics and system integration through manufacturing production:

1. Agilent Technologies' JS-1000 Performance Jitter Solution uses phase noise analysis to measure jitter with unprecedented sensitivity and dynamic range from very low data rates to beyond 40 Gb/s. It is the ideal tool for an R&D environment where thorough understanding of the sources and spectrum of jitter are required and provides complete SONet/SDH/OTN jitter compliance testing.

2. Agilent Technologies' 71501D Jitter Analysis System uses an advanced sampling technique and is a dedicated jitter analysis tool for data rates from 50 Mb/s to 12.5 Gb/s. As a diagnostic tool it provides the demodulated jitter signal in both the time and frequency domains. When accompanied by a bit error ratio tester, it automatically measures jitter transfer and tolerance to SONet/SDH/OTN specifications. The 71501D is also a key component in 10 Gigabit Ethernet optical compliance testing.

3. Agilent Technologies' OmniBER Communications Performance Analyzer uses real-time phase detection to perform compliance testing of network elements to SONet/SDH/OTN specifications. The test suite includes jitter generation and automated sweep measurements of jitter tolerance and transfer at standard rates up to OC-192 and G.709.

4. Agilent Technologies' 86100 Infiniium Digital Communications Analyzer (DCA) equipped with optical and/or electrical receivers is a sampling oscilloscope that provides a wide variety of convenient, quick, visual tools for a variety of eye diagram analyses. It can be used to see the evolution of jitter generation and peculiarities in eye diagrams and pulse shapes. The data acquired by the DCA can be indirectly analyzed to separate deterministic and random jitter.

5. Bit Error Ratio Testers (BERTs) such as Agilent's 86130, 71612C, and 81250 can also be used for jitter analysis by measuring the Bit Error Ratio (BER) as a function of the sampling point position, BER(t), from which random and deterministic jitter can be extracted.

The SONet/SDH/OTN standards and specifications[3] that are repeatedly referred to in this document primarily refer to ITU-T 0.172 and G.709 and Bellcore GR-253-CORE. The Gigabit Ethernet and 10 Gigabit Ethernet standards and specifications[4] primarily refer to IEEE 802.3z and 802.3ae, respectively.

This paper is organized as follows. Section 2 (pg. 2) includes a concise description of jitter and the primary issues in jitter analysis at high data rates. In Section 3 (pg. 10) the five analysis techniques are detailed, and in Section 4 (pg. 23) the techniques are distinguished and recommendations are made for their application.

2. Jitter

The standard definition[5]: Jitter is the short term variation of the significant instants of a digital signal from their ideal positions in time. It is typically concerned with non-cumulative variations above 10 Hz. Cumulative phase variations below 10 Hz are usually defined as *wander*. Figure 1 provides an example of sinusoidally varying jitter.

2.1 Fundamentals of jitter analysis

Jitter is fundamentally an expression of phase noise. Mathematically, jitter is the undesired variation in the phase of a signal given by the term, $\varphi(t)$, in the expression

$$S(t) = P(2\pi f_d t + \varphi(t))$$

where S is the received signal, P represents the sequence of signal pulses as a function of time, and f_d is the data rate. Where $\varphi(t)$ can be measured in radians or degrees, jitter is measured in seconds or unit intervals. The relationship between jitter, J, measured in seconds or Unit Intervals (UI) and phase variation, $\Delta\varphi$, measured in radians, is

$$J\,[\mathrm{s}] = \frac{1}{2\pi f_d}\Delta\varphi\,[\mathrm{rad}] \quad \text{or} \quad J\,[\mathrm{UI}] = \frac{1}{2\pi}\Delta\varphi[\mathrm{rad}]$$

Phase noise and frequency noise and, therefore, jitter, are intimately related. The phase of the signal is given by $\Phi(t) = 2\pi\ f_d t + \varphi(t)$, so the frequency is given by

$$f(t) = \frac{1}{2\pi}\ \frac{d}{dt}\Phi(t) = \ f_d + \frac{1}{2\pi}\ \frac{d}{dt}\ \varphi(t).$$

The frequency noise is

$$\Delta f(t) = f(t) - f_d = \frac{1}{2\pi}\ \frac{d}{dt}\ \varphi(t)$$

showing that a measurement of jitter, or phase noise, includes the measurement of frequency noise. The coordinate system and many of the terms used in this paper are defined in the eye diagram of Figure 2.

Figure 1. Comparison of an ideal clock and a sinusoidally jittered clock. The jitter amplitude is ⅔ UI.

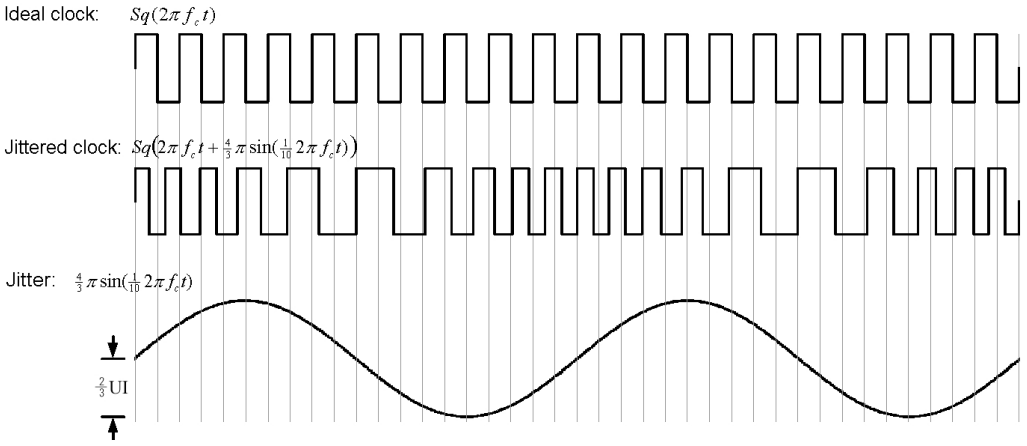

Figure 2. Eye diagram with definition of terms.

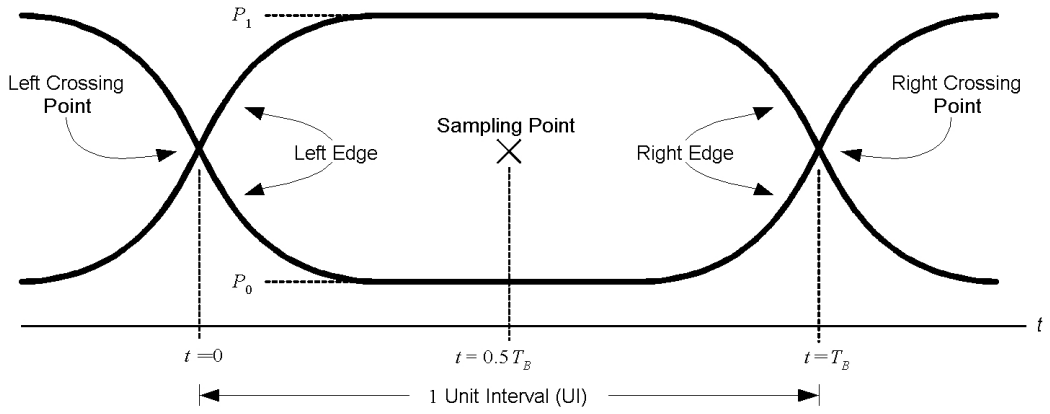

2.1.1 Jitter generation

Jitter generation, or intrinsic jitter, is jitter *generated* by a component, i.e., the output jitter of a component when the input has no jitter. It is usually represented by two quantities: peak-to-peak, J_{pp}, and rms, J_{rms}, jitter. Jitter generation results from a combination of random jitter and deterministic jitter.

Random jitter (RJ) is the jitter generation from the accumulation of random processes including thermal noise and shot noise. It is generally assumed to follow a Gaussian distribution which is characterized by a mean, μ, and a width, σ, as shown in Figure 3. In the absence of deterministic jitter, RJ determines the position of an edge. The probability that the edge crosses the sampling point, causing a bit error, follows a Gaussian distribution. The width of the distribution is the contribution of random jitter to the total rms jitter: $J_{rms}^{RJ} = \sigma$. Since the tails of a Gaussian distribution extend to infinity, the peak-to-peak value of RJ, J_{PP}^{RJ}, is unbounded. This means that the longer J_{PP}^{RJ} is measured, the larger it gets; whereas J_{rms}^{RJ} should only vary about its true value during a measurement.

Deterministic jitter (DJ) is the jitter generation from a variety of systematic effects. The causes include duty-cycle-distortion (DCD), intersymbol interference (ISI), sinusoidal or periodic jitter (PJ), and crosstalk. DCD results from asymmetries in clock cycles, for example, differences in rise and fall times. ISI results from variations in edge response due to phenomena such as dispersion or data dependent effects, for example, when a logic "1" follows a long string of "0"s. PJ results from periodic pickup from other periodic sources, for example, power supply feedthrough. Crosstalk is caused by pickup from other signals including electromagnetic interference. The distinguishing feature of DJ is that its peak-to-peak value is bounded where the peak-to-peak value of RJ can be arbitrarily large. In terms of RJ and DJ, it is useful to characterize the total jitter of a system as a combination of the peak-to-peak DJ value, J_{PP}^{DJ}, and the rms RJ value, J_{rms}^{RJ}.

To develop an intuition for RJ and DJ, consider Figure 4 where there are several distinct pulse shapes. The different pulse shapes are caused by DJ. The width of the lines is determined by RJ. That is, DJ determines which line a given bit will follow and RJ determines how much that bit oscillates about the DJ determined average. J_{PP}^{DJ} is given by the distance between the most widely separated DJ determined edges, and J_{rms}^{RJ} is the rms deviation about a given edge. DJ does not usually provide such distinct edges as those in the eye diagram of Figure 4.

A useful design approach common in Gigabit Ethernet applications is to restrict the total peak-to-peak jitter to a given jitter budget. But interpreting a measurement of peak-to-peak jitter can be confusing. Accurate measurements of jitter require a large data sample, but since RJ is a Gaussian process, its peak-to-peak value increases with sample size. This makes the value of J_{PP}^{RJ} ambiguous. To avoid this ambiguity two approaches are common: SONet/SDH/OTN engineers measure J_{PP} over a specified time interval. Gigabit Ethernet and Fibre Channel engineers use the fact that, in the absence of DJ, the width of the RJ distribution, σ, determines the Bit Error Ratio (BER) and define J_{PP}^{RJ} to correspond to a specific BER. Table 1 shows

Figure 3. An eye diagram with Random Jitter (RJ) showing the effect of RJ on BER.

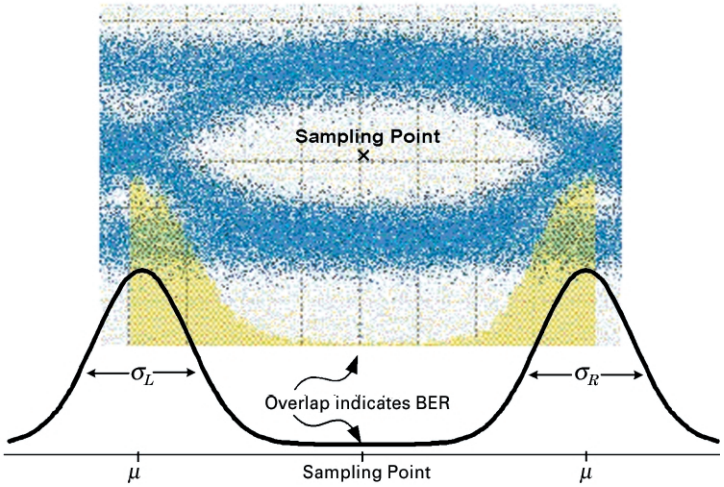

Figure 4. An eye diagram with both Random Jitter (RJ) and Deterministic Jitter (DJ) distinguishing the genuine rms jitter, from the rms jitter caused by RJ, J_{rms}^{RJ}, and the total peak-to-peak jitter, J_{PP}, from the peak-to-peak jitter caused by DJ, J_{PP}^{DJ}.

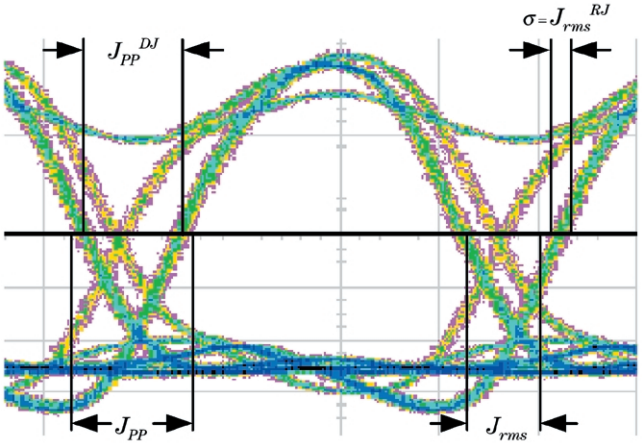

the relationship between peak-to-peak and rms values of RJ in the absence of DJ or other noise sources. It is reasonable to define J_{PP}^{RJ} in multiples of $\sigma = J_{rms}^{RJ}$ so that it corresponds to a given BER in the absence of DJ. You can then combine J_{PP}^{RJ} and J_{PP}^{DJ} to get a total peak-to-peak jitter for comparison to the combination of a jitter and BER budget:

$$\begin{aligned} J^{TJ} &= n \times \sigma \quad + J_{PP}^{DJ} \\ &= n \times J_{rms}^{RJ} \; + J_{PP}^{DJ} \end{aligned} \tag{1}$$

If J_{PP} is measured without separating RJ and DJ, then the RJ component is probably a genuine peak-to-peak measurement that will grow as the data sample increases and won't be defined according to Table 1. J_{PP} and J_{PP}^{DJ} as well as J_{rms} and J_{rms}^{RJ} are distinguished in Figure 4 (pg. 3). The genuine peak-to-peak jitter, J_{PP}, despite the ambiguity, is a very useful quantity because large values indicate error-causing events. In SONet/SDH/OTN applications the requirements on J_{PP} are frequently the most difficult to meet.

Random jitter and some types of deterministic jitter can have different values when measured over different bandwidths. To understand this consider thermal noise, the dominant source of RJ. Like any white noise, it tends to be constant across the frequency spectrum. Thus the measured value depends on the bandwidth over which it is measured. SONet/SDH/OTN specifies the bandwidth over which jitter must be determined, but different test and measurement equipment may not limit the band to these ranges. For example, the bandwidths of sampling oscilloscopes are very large and will measure jitter over correspondingly large bandwidths. When measuring jitter against a specification with a jitter test set it is important to use standard-specific filters to limit the bandwidth appropriately; for jitter measurements with sampling oscilloscopes or Bit Error Ratio Testers the jitter bandwidth is not easily limited.

Transmitters are dominant contributors of RJ. The majority of jitter generated by an externally modulated laser transmitter is due to random noise from the lasers and the master reference clock. Conversely, the majority of jitter generated by a receiver is DJ, due to things like AC coupling of the preamp and postamp connection causing ISI. Directly modulated laser transmitters suffer from both RJ and DJ. The medium can go either way: optic fibers can contribute DJ from dispersive effects and RJ from a variety of scattering effects; conducting media tend to be dominated by DJ because their finite bandwidths attenuate higher frequencies more than lower.

Table 1. The relationship between BER and peak-to-peak values of random jitter, $\sigma = J_{rms}^{RJ}$.

Bit Error Ratio (BER)	Peak-to-Peak RJ $J_{PP}^{RJ} = n \times \sigma$
10^{-10}	$12.7 \times \sigma$
10^{-11}	$13.4 \times \sigma$
10^{-12}	$14.1 \times \sigma$
10^{-13}	$14.7 \times \sigma$
10^{-14}	$15.3 \times \sigma$

2.1.2 Jitter transfer and jitter tolerance

Jitter transfer measures the clock recovery performance of a network or network element as a function of jitter frequency. It is measured by applying sinusoidal jitter of specified amplitude and frequency, $\varphi(t) = A_{Appl} \sin(2\pi f_J t)$, to the data and measuring the output jitter amplitude at that frequency, $A_{out}(f_J)$. The jitter transfer is given by $X_{Tfer}(f_J) = A_{out}(f_J) / A_{Appl}(f_J)$.

Jitter tolerance measures the ability of a device or system, primarily at the receiving end, to track large amounts of jitter without degrading the BER. It is the amplitude of sinusoidal jitter applied to a device that results in an equivalent 1 dB reduction in sensitivity. The measurement is performed by first measuring the BER of the Device Under Test (DUT) without applied jitter. The signal power is attenuated until the onset of errors or until a specified BER, typically 10^{-12}, is exceeded. The attenuation is reduced 1 dB and the signal is transmitted with applied sinusoidal jitter $\varphi(t) = A_{Appl} \sin(2\pi f_J t)$, imposed on the clock. The jitter amplitude is increased until the onset of errors or the specified BER is exceeded. The resulting jitter amplitude is the jitter tolerance at that frequency, $A_{Tol}(f_J)$.

Jitter tolerance and transfer are primarily of interest in SONet/SDH/OTN applications.

2.2 Jitter in SONet/SDH/OTN applications

SONet, SDH, and OTN, as synchronous protocols, depend strongly on the relative timing of accurate stable clocks. The emphasis is less on jitter generation than on the propagation of jitter through the network. Jitter analysis in SONet/SDH/OTN focuses on contributions of jitter in the frequency domain. The measurements are band-limited and separate requirements are made of jitter and wander.

In SONet/SDH/OTN jitter generation compliance is based on band limited peak-to-peak and rms values without separating jitter generation into its RJ and DJ components. The peak-to-peak jitter generation measurement, J_{PP}, is the genuine peak-to-peak value, although it is sometimes given, for reasons similar to those in reference to Table 1, as $6 \times \sigma$ (the factor of six is called a "crest-factor"). In SONet/SDH/OTN the payload is scrambled to prevent long strings of logic zeros or ones, but the frame header is not scrambled. The resulting data-dependent DJ can dominate the system. Thus accurate measurement of J_{PP} is key to the characterization of these networks. To provide repeatable measurements, band limiting is performed by submitting the signal to a bandpass filter centered at the data frequency. The filter bandwidth and center frequency are specific to each data rate. The generic requirement is for $6 \times \sigma$ jitter to be less than 10% of the bit period (100 mUI).

Figure 5. The basic elements of a jitter analysis system including the components necessary for jitter tolerance and transfer measurements.

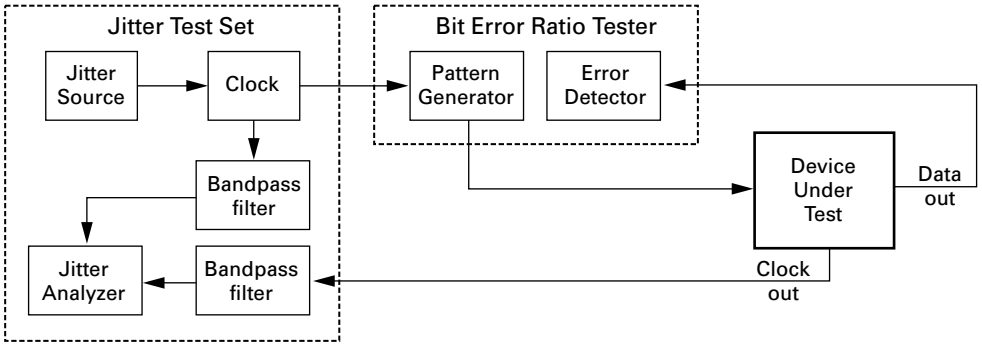

Figure 6. (a) OC-48 jitter transfer and (b) jitter tolerance examples, including masks.

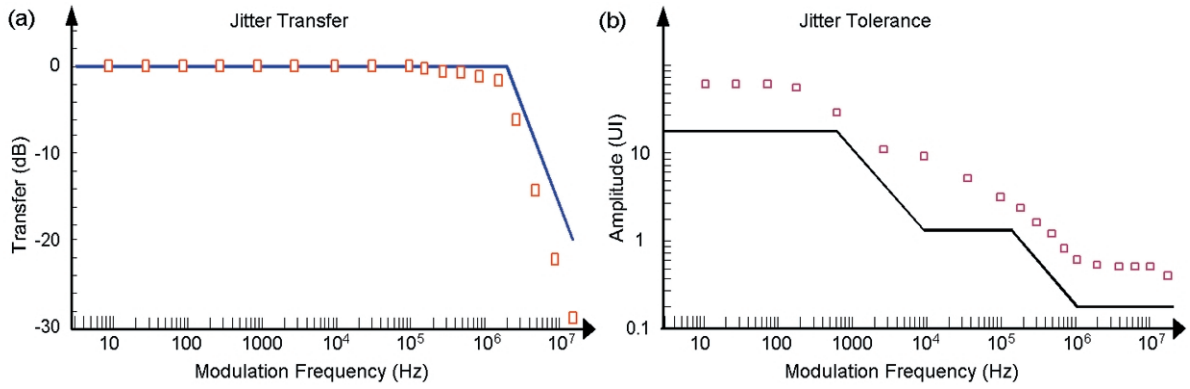

To measure jitter transfer, a jitter source, as shown in Figure 5 (pg. 5), is applied to the clock. The clock defines the timing of data from the pattern generator. This data is provided to the DUT. To measure jitter transfer and tolerance, the jitter source must be capable of applying sinusoidal jitter, $A_{Appl} \sin(2\pi f_J t)$, with amplitudes, A_{Appl}, at least as large as those required by the specification. In SONet/SDH/OTN jitter transfer measurements, the required amplitudes of applied sinusoidal jitter follow a template with large amplitudes for low frequencies and small amplitudes for high frequencies. It is also useful to stress a DUT with other jitter waveforms (e.g., triangle wave, square wave, or random noise) to further understand the DUT's jitter response. The SONet/SDH/OTN jitter transfer requirements are provided as masks for different transmission rates, an example is shown in Figure 6a (pg. 5) for OC-48 (2.488 Gb/s). If the graph of X_{Tfer} vs. f_J is below the mask then the system is in compliance.

To measure jitter tolerance, the data output of the DUT is provided to the error detector of a Bit Error Ratio Tester (BERT), also in Figure 5 (pg. 5). The SONet/SDH/OTN jitter tolerance requirements are also provided as masks, Figure 6b (pg. 5). If the graph of A_{Appl} vs. f_J is above the mask then the system is in compliance. The margin by which the jitter tolerance of a system exceeds the specification can be measured by increasing the amplitude of applied jitter at each frequency until the onset of errors or until a given BER is exceeded. This is a jitter tolerance search.

2.3 Jitter in Gigabit Ethernet applications

Jitter analysis in both Gigabit and 10 Gigabit Ethernet is predicated on restricting jitter generation. Since Ethernet is not a synchronous network there are no explicit jitter transfer or tolerance requirements. However, understanding the transfer and tolerance of network elements is useful in the design of and for debugging components in Gigabit Ethernet applications. There are requirements for phase locked loop bandwidth that are similar in spirit to jitter transfer that are indirectly tested in the stressed eye receiver test. The measurements are not band-limited so the jitter measurements implicitly include low frequency/near-carrier wander.

2.3.1 Gigabit Ethernet

Jitter requirements for 1 Gigabit Ethernet were modeled after and are similar to the Fibre Channel specifications. A total jitter (TJ) budget is provided and then fractions of it are allocated to different parts of the system. The TJ is the sum of the peak-to-peak DJ and RJ as defined in section 2.1.1. so that $J^{TJ} = J_{PP}^{DJ} + n \times J_{rms}^{RJ}$. DJ is defined for certain data patterns, circuitry, and transmission media. The standard approach for separating RJ and DJ to determine the jitter margin of a device is described in Section 3.5 (pg. 20). It uses a Bit Error Ratio Tester (BERT) to derive the *Bathtub Plot*, i.e., the BER dependence on the time position of the sampling point, BER(t). RJ and DJ, and to some extent, different contributors of DJ, can be distinguished through analysis of the bathtub plot.

2.3.2 10 Gigabit Ethernet

In the 10 Gigabit Ethernet specification jitter is not directly measured. Instead, separate requirements are made of transmitters and receivers.

For transmitters, the specification limits the *Transmitter Dispersion Penalty* (TDP). TDP is the level of attenuation that must be applied to a transmitter in a dispersive link to increase the BER to the level of a reference receiver in a non-dispersive link whose sampling point is dithered ±5 ps. TDP is ultimately a method for limiting jitter generation.

For receivers, a *stressed eye receiver sensitivity* test is performed. The test is designed to verify that a receiver can operate at a BER of better than 10^{-12} when receiving the worst case allowable signal. The test signal is designed to simulate a variety of stresses including RJ, DJ, interference, and attenuation. This test is analogous to jitter tolerance. Both RJ and DJ are applied in specified magnitudes to characterize the receiver against the worst-case jitter from a compliant transmitter. The test system must be able to generate more than the maximum allowed transmitter jitter. It consists of a combination of applied sinusoidal jitter and filtering to simulate DJ, Figure 7. A 1-2 GHz, sinusoidal interference signal is added (not mixed!) to the pattern to simulate RJ and vertical eye closure.

The applied levels of RJ and DJ are given for 10 Gigabit Ethernet without a specific method for how they should be generated. Similar to SONet/SDH/OTN, the amplitude of applied sinusoidal jitter follows a template with large amplitudes for low frequencies and small amplitudes at high frequencies. Random jitter can also be simulated through noise injection and data dependent jitter by adding lengths of coaxial cable, or inserting a low pass filter before the test system transmitter.

The margin of compliance can be measured by further stressing the eye. All elements of the stressed eye test can be set independently, e.g., the simulated RJ or DJ can be switched in and out; the sinusoidal jitter amplitude can be adjusted to determine the robustness of the device under test; and the attenuation and sinusoidal interference can be tuned. In addition to performing these qualitative tests of jitter, essentially characterizing horizontal eye closure, the stressed eye test set also includes simulation of optical noise for vertical eye closure.

Figure 7. Block diagram of the stressed eye receiver test.

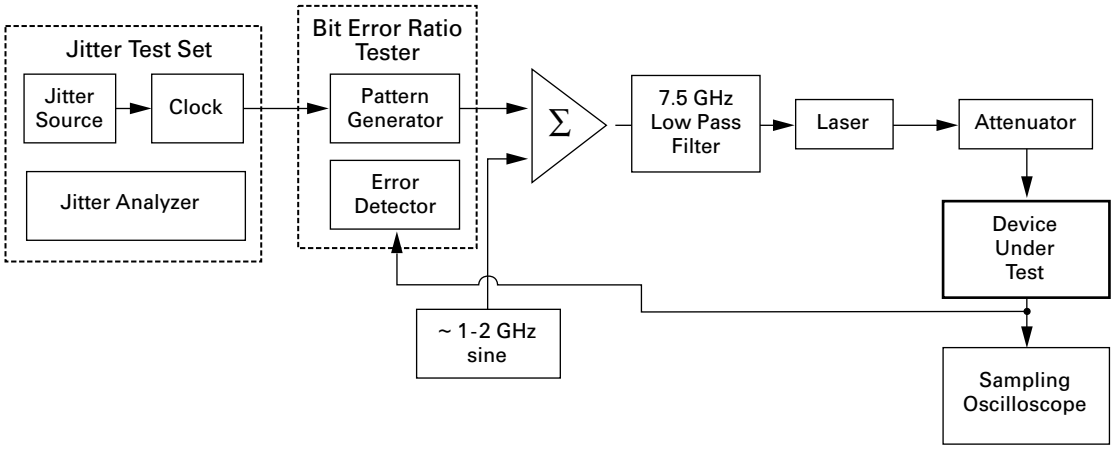

2.4 Uncertainty in the measurement of jitter

The accuracy of a jitter measurement is limited by two properties of the test system: its noise floor, J_{NF}, and its repeatability, R. The noise floor is jitter generated by the system and is also referred to as the receiver intrinsic jitter or the test equipment fixed error, W, in reference 3 (pg. 28). The repeatability is the uncertainty† of a given measurement. It is the range of values that a given measurement may fall within, $J_{truth} = J_{meas} \pm R$. It is usually proportional to the measurement and is given in percent, in this case, $J_{truth} = J_{meas}\,(1 \pm 100 \times R)$. The noise floor combined with the repeatability limits the lowest jitter level that the test system can consistently measure. Making a few standard assumptions from statistical theory—that measurements follow a Gaussian distribution centered on the true value with a width that is roughly one third of the repeatability—then a given measurement is distinguishable from noise with a confidence level of 95% if the measured jitter generation, J, obeys [6]

$$J > R\sqrt{1 + \frac{9J_{NF}^2}{R^2}} \quad \text{(for } R \text{ in seconds or UI)}$$

$$J > \frac{3J_{NF}}{\sqrt{1 - (100 \times R)^2}} \quad \text{(for } R \text{ in percent).} \qquad (2)$$

Equation (2) determines the minimum jitter generation measurement that a system can perform. For example, if it is necessary to consistently measure jitter of 0.100 UI (J_{min}) and the measurement repeatability is R = 10%, then the jitter generation of the test system must be on the order of J_{NF} < 0.035 UI. If a measurement, J, is within R of the noise floor, then the actual jitter generation of the DUT is less than the measured value (with about 95% confidence). Neither the noise floor nor the repeatability can be calibrated out of the measurement. Since jitter is broadband noise, the noise floor depends on the bandwidth of the measurement.

In jitter transfer measurements the noise floor is reduced because the measured jitter bandwidth is limited to a small range centered on the applied jitter frequency. Further, since transfer is the ratio of the received to transmitted jitter amplitude, much of the uncertainty due to the transmitter cancels. However, the applied jitter amplitude can be large and the received jitter amplitude can vary widely depending on the character of the DUT. For example, the output amplitude of jitter from a narrow bandwidth device is larger when the applied jitter frequency is in the passband. The repeatability of jitter transfer measurements is also usually proportional to the measured transfer.

Results from different methods can only be compared if their uncertainties are understood. Inconsistent comparisons of jitter measurements between different test systems are caused by differences in the noise floor and repeatabilities of the systems, but they can also be caused by systematic differences in the test techniques. For example, two techniques described below, measurement of jitter with a sampling oscilloscope (DCA) and a bit error ratio tester have completely different systematic uncertainty than the other techniques.

† *There is no standard industry definition for 'measurement uncertainty' in terms of the distribution of a set of repeated measurements. Agilent Technologies reports at least 95% confidence intervals for measurement uncertainty. In this paper we use a conservative approach and assume that the uncertainty is defined so that 95% of all measurements fall within one unit of repeatability of the true value.*

2.5 The role of clock recovery circuits in jitter measurements

Jitter is always measured with respect to an idealized time scale that is almost always implemented as a low noise reference clock, as indicated in Figure 5 (pg. 5). Measuring jitter on DUTs that do not include Clock Recovery (CR) or Clock Data Recovery (CDR) circuits can be complicated. To measure jitter generation and transfer on a data signal (but not tolerance), a CR circuit that passes the DUT jitter must be inserted between the DUT data output and the jitter test system. To transparently pass the DUT jitter, the CR must have:

1. very low jitter generation so that the noise floor of the system is not increased beyond the level necessary for useful testing—recommend $J_{CR} < 3\ J_{NF}$
2. a bandwidth large enough to pass jitter of the maximum jitter frequency of interest and,
3. a flat transfer function to avoid distorting the DUT jitter.

Since *frequency agile* CRs and CDRs that meet the three requirements are not readily available, the two frequency agile systems described below, the Agilent JS-1000 and 71501D, require external CR circuits at the desired clock rate to measure jitter on data-only signals. The OmniBER has a specially designed CR to provide clock signals at specific standard rates.

The jitter generation of the CR increases the noise floor of the test system and cannot be calibrated out of the measurement. Consider the rms jitter generation of the DUT and CR under the assumption of a perfect measurement system. The two can be combined by using the covariance of the system,

$$J_{meas}^2 = J_{DUT}^2 + J_{CR}^2 + \rho\, J_{DUT}\, J_{CR}$$

The correlation of the CR and DUT, ρ, describes the way that the CR reacts to the DUT jitter. If the jitter of the DUT and CR were independent, then $\rho = 0$ and it would be easy to separate the CR and DUT jitter. But the jitter of the two systems interferes in complicated ways that make it impossible, in practice, to measure ρ. It is therefore necessary to maintain a very low jitter CR: $J_{CR}/J_{DUT} << 1$ so that $J_{DUT} = J_{meas} \pm R$.

In some cases it is possible to measure the RJ and some of the DJ on devices without recovered clocks by driving them with a high clock content signal, such as an alternating pattern: 10101010.... For such a signal, the DUT output mimics a clock signal and will pass all jitter that is independent of the data pattern. This measurement will *not* include DJ contributions from pattern dependent jitter, some contributions from periodic jitter, and crosstalk that may diversely affect different pattern sequences. The deviation of the phase—the jitter amplitude—in this measurement is cut in half but the jitter frequency doesn't change. Thus, in a band limited measurement, even though the data rate, f_d, is half the clock rate, $2 \times f_d$, the same filters used to band limit the measurement at the full clock rate should be used.

For *jitter transfer* measurements the bandwidth of the CR must be larger than the highest jitter frequency applied. In this measurement, the test system applies sinusoidal phase noise (i.e., phase modulation) to the system, $J_{applied}(t) = A \sin(2\pi\ f_J t)$. The effect of the DUT is to change the amplitude so that, $J_{DUT}(t) = A' \sin(2\pi\ f_J t) + J_g(t)$, where $J_g(t)$ is the jitter generation contribution of the DUT. As long as the amplitude of the applied jitter is much larger than the jitter generation of the CR, Figure 8 (pg. 5)—which should always be the case—then the response of the DUT to the applied jitter dominates the measurement and an accurate transfer measurement can be performed.

The situation is quite different for clock recovery in most system components where the CR circuits require a narrow bandwidth to maintain the integrity of network timing.

For measurements of *jitter tolerance* the situation is also different. The goal of jitter tolerance is to measure the ability of a receiver to track jitter without degrading the BER. The data output of the DUT goes directly to the BERT error detector, as shown in Figure 5 (pg. 5). To synchronize and align with the data, the error detector also requires a clock signal. Since tolerance is meant to measure how robust the system is to jitter, a jitter-free system clock is needed, but the clock driving the BERT pattern generator is modulated with an applied jitter signal. Thus, for measuring jitter tolerance on a data-only signal, a *narrow bandwidth* low noise CR is required.

Figure 8. Effect of a Clock Recovery (CR) circuit's jitter generation on the measurement of jitter transfer.

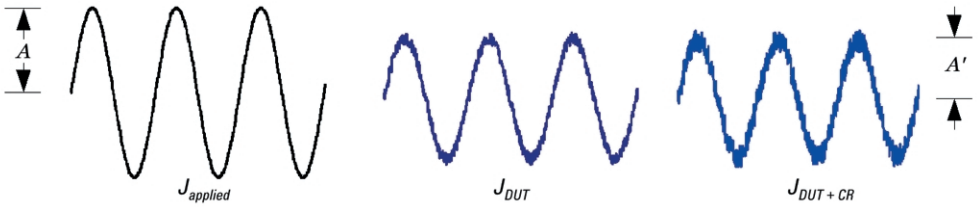

3. Jitter analysis

At high data rates the only real-time technique that is possible with current technology is analog based phase detection. Other approaches rely on sampling techniques. A disadvantage of sampling techniques is that, since they don't measure the phase variations of every bit, they can miss transient phenomena. Agilent provides both real time, the (JS-1000 and OmniBER) and sampling techniques (the 71501D and 86100) as well as indirect digital techniques that use bit error ratio testers.

3.1 High performance phase noise analysis— The JS-1000.

3.1.1 Application focus

The JS-1000 is the industry's highest performance jitter analysis system. It is a tailored phase noise system that measures jitter characteristics of clock signals in the data rate ranges: 2.4 - 3.125 Gb/s, 9 - 13 Gb/s, and 38 - 45 Gb/s and can be customized for analysis at additional data rates. The JS-1000 can be ordered with low jitter generation, flat jitter transfer, wide bandwidth clock recovery (CR) interfaces for certain data rates, as described above in Section 2.5, (pg. 9) for characterization of jitter generation and transfer on data-only signals.

The JS-1000 is an R&D design tool with a remarkably low noise floor. It can measure jitter generation, tolerance, and transfer well beyond compliance to the SONet/SDH/OTN standards and can be integrated into a stressed eye receiver test set, Figure 7 (pg. 7). It does not permit RJ-DJ separation similar to the techniques commonly used in Gigabit Ethernet/Fibre Channel analyses; however, as described below, analysis of $\varphi(t)$ can identify specific contributions from different DJ sources and distinguish different types of RJ within the bandwidth of the phase noise analyzer. A model of the jitter can be developed based on a few assumptions from the phase noise data. The ability to identify jitter sources at this level is a valuable tool for streamlining product design and solving jitter problems.

3.1.2 Phase noise analysis of jitter

Phase noise analysis[7] is a precise technique performed in the frequency domain. A phase detector (mixer) removes the carrier and extracts the phase noise from the signal with an accuracy limited by the phase noise of the reference clock. As shown in Figure 9, the inputs to the mixer are a reference clock, $V_{ref}(t) = A_{ref}\sin(2\pi f_d\, t + \pi/2)$ and the DUT clock, $V_{DUT}(t) = A_{DUT}\sin(2\pi f_d\, t + \varphi(t))$. The relative phase of the reference clock, $\pi/2$, is maintained by the phase shifter following the reference clock prior to the mixer. The output that follows the low pass filter is $V(t) = K_\varphi \sin(\varphi(t))$. For small phase variations ($\Delta\varphi << 1$ rad) we use $K_\varphi \sin(\varphi(t)) \approx K_\varphi \varphi(t)$. K_φ is the phase to voltage conversion factor in V/rad. The output of the phase detector is provided to a spectrum analyzer from which the phase spectral density

$$S_\varphi(f) = \frac{1}{K_\varphi^2}\,\frac{\Delta V_{rms}^2(f)}{\Delta f} = \frac{\Delta\varphi_{rms}^2(f)}{\Delta f}\left[\mathrm{rad}^2/\mathrm{Hz}\right]$$

can be extracted. Here, f is the frequency of the phase noise component, $S_\varphi(f)$ is the mean square phase variation, $\Delta\varphi_{rms}^2(f)$, over the frequency interval, or bandwidth, Δf. An oscilloscope is included in the JS-1000 system for measuring peak-to-peak jitter and large amplitude jitter (e.g., $\Delta\varphi > 2\pi$ rad).

A similar way to remove the carrier and extract the phase noise is to use the Single Side Band (SSB) power referenced to the carrier frequency, $\mathcal{L}(f)$. If the signal, $V_{DUT}(t) = A_{DUT}\sin(2\pi\, f_d\, t + \varphi(t))$, is directed to a spectrum analyzer, the spectrum is composed of a strong signal at the carrier frequency with sidebands caused by phase fluctuations. The SSB phase noise, $\mathcal{L}(f)$, can be extracted from the spectrum,

$$\mathcal{L}(f) = \frac{1}{2P_C}\,\frac{\Delta P(f)}{\Delta f} = \frac{\text{Power density of one phase modulation sideband}}{\text{Carrier Power}}$$

Figure 9. Phase noise analysis system.

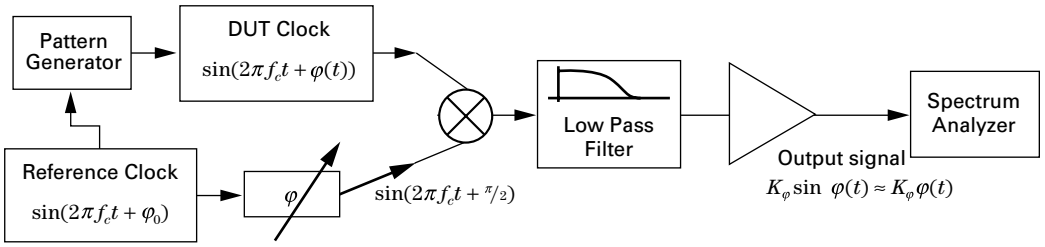

It is shown in Appendix A that

$$\mathcal{L}(f)\ \left[{}^{1}/_{\mathrm{Hz}}\right] = \tfrac{1}{2} S_{\varphi}(f)\left[{}^{\mathrm{rad}^2}/_{\mathrm{Hz}}\right] \tag{3}$$

The SSB spectrum extracted from a spectrum analyzer suffers from two defects compared to the phase noise spectrum, measured by a phase detector. First, as shown in Appendix A, amplitude noise contributes to the SSB spectrum. To accurately extract jitter from the SSB spectrum the amplitude noise contribution must be much less than 20 dB below the phase noise contribution. Second, the filter shape of the spectrum analyzer allows some of the high magnitude noise close to the carrier to leak through, distorting the SSB spectrum from the actual phase noise spectrum. A general purpose electrical spectrum analyzer is quite useful for observing jitter through the SSB spectrum, but may not provide the performance necessary to fully characterize jitter performance and isolate jitter problems.

Equation (3) gives the square of the phase noise magnitude per unit frequency interval measured over some time period, $\Delta\varphi^2_{rms}(f)/\Delta f$. Thus, the rms jitter generation (in radians) can be extracted by integrating $\mathcal{L}(f)$, for example in Figure 10, over the desired bandwidth:

$$J_{rms} = \sqrt{\int_{f_1}^{f_2} \frac{\Delta\varphi^2_{rms}(f)}{\Delta f}\, df} = \sqrt{\int_{f_1}^{f_2} S_{\varphi}(f)\, df} = \sqrt{\int_{f_1}^{f_2} 2\mathcal{L}(f)\, df} \tag{4}$$

The key to identifying significant contributions of DJ from the phase noise plot is to consider only those spurs in the spectrum that contribute appreciably to the jitter generation extracted by integrating Eq. (4). The JS-1000 integrates whatever combination of spurs and smooth background in the phase noise spectrum that the user desires.

Different types of deterministic jitter can be identified and separated by analyzing the phase noise spectrum, $\mathcal{L}(f)$. Consider the spectrum shown in Figure 10; the peak at the very low end of the spectrum is from small fluctuations near the carrier, the spurs and harmonics from 60 Hz pick-up are clearly visible at the low end, there is a broad background contribution from about 100 Hz to about 1 MHz, and there is an obvious structure around 5 MHz at the higher end. A repeating data pattern, such as a Pseudo Random Binary Sequence (PRBS) causes narrow spurs in the spectrum at the repetition rate and its harmonics.

Figure 10. Single side band phase noise spectrum.

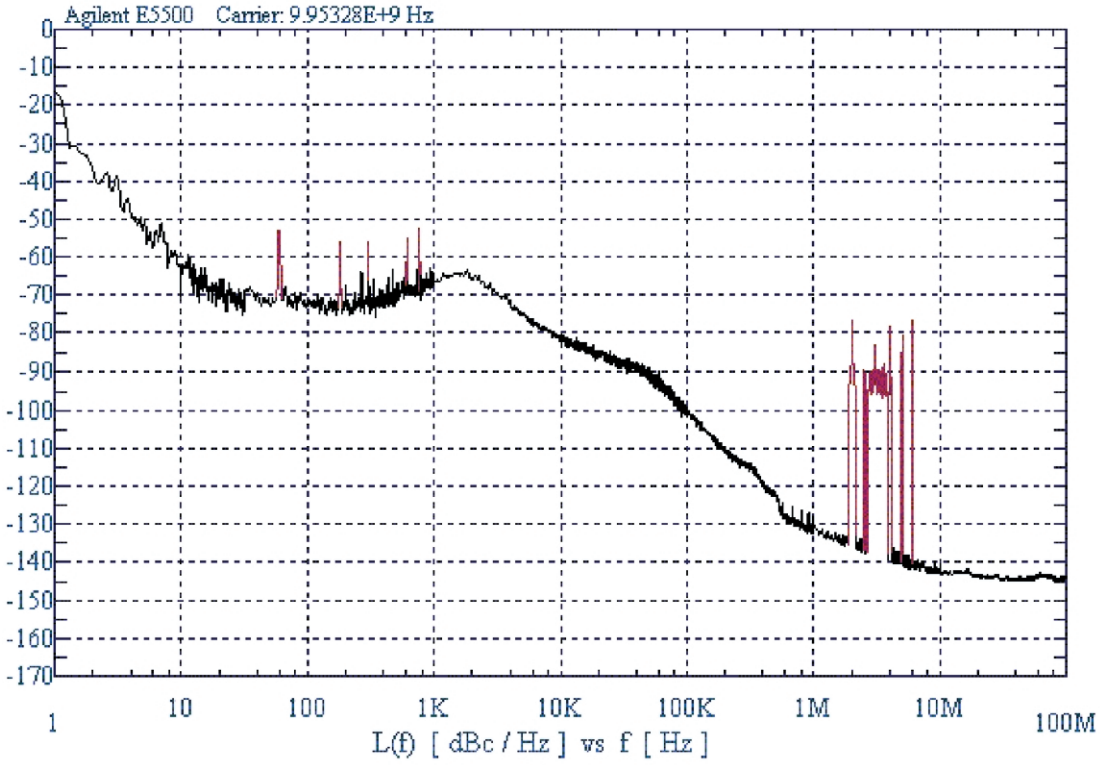

The 60 Hz pick-up is an example of how periodic DJ causes spurs at the period frequency and its harmonics. The contributions of RJ and DJ to $\mathcal{L}(f)$, within the frequency band of the phase noise spectrum, can be understood in an offline analysis by fitting a model of the random processes that contribute to the phase noise, e.g., a power law noise model[8]

$$\mathcal{L}_{Random}(f) = \sum_{n=\infty}^{\infty} h_n f^n \qquad (5)$$

where h are coefficients of different frequency terms. The phase noise spectrum is usually dominated by five terms: $n = -2$, random walk FM; $n = -1$, flicker FM; $n = 0$, white FM; $n = 1$, flicker PM; and $n = 2$, white PM. The coefficients can be derived by fitting Eq. (5) to the measured spectrum. Deviations from the smooth fitted curve indicate the behavior of DJ contributors in the frequency domain.

Peak-to-peak jitter generation is measured by the JS-1000 through accumulation of bit-by-bit phase deviations. Since RJ is unbounded, the peak-to-peak jitter generation increases without bound with the number of measurements. The real-time measurement of the JS-1000 demonstrates this by yielding peak-to-peak measurements derived from every bit and a correspondingly larger peak-to-peak measurements than a sampling method would obtain over the same time interval. Two examples of jitter histograms accumulated by the JS-1000 are shown in Figure 11. Figure 11a shows the jitter histogram of a device with large deterministic jitter—it obviously does not follow a Gaussian distribution. Figure 11b shows a histogram of a device with very little deterministic jitter but is stimulated by a PRBS pattern. A low level of data dependent deterministic jitter distorts the signal from a Gaussian shape due to repetition of the PRBS pattern.

3.1.3 The JS-1000 system

The JS-1000 is a jitter analysis system based on Agilent's E5510 phase noise system with additional reusable equipment: a phase modulation generator, a low phase noise microwave spectrum analyzer, a microwave source, 100 MHz digitizing oscilloscope, and a 10 MHz FFT baseband analyzer. Since the system measures jitter on a clock signal it is ideal for characterizing Phase Locked Loops (PLLs), Voltage Controlled Oscillators (VCOs), amplifiers, and Clock Data Recovery (CDR) circuits. An additional BERT, such as the Agilent 71612C is necessary for measuring jitter tolerance.

Jitter generation is extracted for a given band of frequencies f_1 to f_2 using Eq. (4) (pg. 12). Jitter transfer and tolerance are measured by applying sinusoidal jitter to the system clock by the phase modulation generator. In jitter transfer measurements, the resulting output jitter is measured at the generated frequency to obtain the transfer function defined in Section 2.1.2 (pg. 12), $X_{Tfer}(f_J) = A_{out}(f_J) / A_{Appl}(f_J)$. Sinusoidal jitter can be applied with amplitudes well above the SONet/SDH/OTN requirements. The JS-1000 has similar template flexibility and margin test features for both jitter transfer and tolerance characterization as the 71501D described below in Section 3.2 (pg. 13). The maximum amplitudes of applied jitter are well beyond those required by the standards:

- 500 kUI for 10 Hz to 10 kHz;
- 500 UI for 10 to 400 kHz;
- 6.25 UI for 400 kHz to 4 MHz;
- 0.625 UI for 4 to 5 MHz; and,
- 0.5 UI for 5 to 80 MHz.

The important specifications are:

- The jitter noise floor is less than 50 μUI and the measurement repeatability (or uncertainty) is ±0.2 dB.
- Jitter transfer is measured with 0.005 dB resolution, ±0.01 dB accuracy to 10 MHz modulation bandwidth and ±0.2 dB accuracy of roll-off to –20 dB, ±0.4 dB accuracy of roll-off to –40 dB.
- Jitter tolerance measurements provide 80 MHz bandwidth of applied jitter to ±0.5 dB accuracy.

Figure 11. Histograms of jitter measured by the JS-1000. In (a) the DUT has large contributions of DJ; and in (b), the DUT has little DJ.

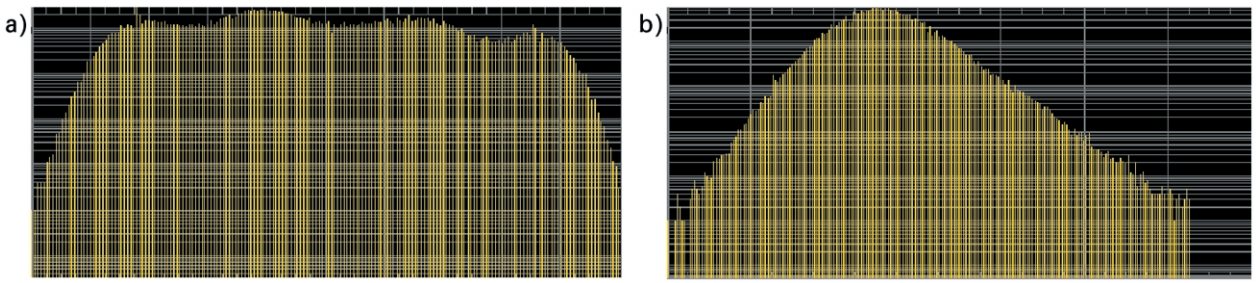

3.2 Microwave transition analysis—The 71501D

3.2.1 Application focus

The 71501D system automatically measures jitter generation, transfer, and tolerance to SONet/SDH/OTN specification, and can be integrated into the stressed eye test set for 10 Gigabit Ethernet component compliance testing. It can measure jitter characteristics at any modulation rate from 50 Mb/s to 12.5 Gb/s. It measures jitter by sampling the clock signal supplied by the device under test (DUT), but can measure jitter from a data-only signal if accompanied by a Clock Recovery (CR) circuit of the appropriate rate, as described in Section 2.5 (pg. 9). Measuring jitter tolerance requires the addition of an Agilent 71603, 86130, or 71612 BERT. It does not separate the jitter generation into its RJ and DJ components, but can display the demodulated jitter signal for identification of DJ frequency terms.

Jitter is measured by microwave transition analysis, a powerful sampling technique. The reference clock and DUT recovered clock are sampled by Agilent Technologies' 70820A Microwave Transition Analyzer (MTA)[9]. The MTA detects both signals with a synchronous, dual channel receiver. The MTA is accompanied by a low phase noise reference clock, such as Agilent Technologies' 83752, a function generator to apply jitter to signals, Agilent Technologies' 33250A function generator, and a modulation test set, Agilent Technologies' N1015A, to complete the 71501D Jitter Analysis system.

By virtue of the sampling technology used in the MTA, the 71501 can optionally be equipped with software to perform eye diagram analyses similar to those performed by a Digital Communications Analyzer like the Agilent 86100.

3.2.2 Microwave transition analysis of jitter

The MTA is a two channel instrument whose bandwidth covers DC to 40 GHz. It acquires a waveform through repetitive sampling of the input. The sampling frequency is internally synthesized, based on the frequency of the input signal and the desired time scale. The sampling frequency is automatically adjusted to achieve a controlled aliasing of the frequency components of the input signal. It is a natural jitter analysis tool for several reasons. First, by correlating the nominal carrier frequency to the sampling frequency, it demodulates the jitter signal to obtain $\varphi(t)$. Second, since the MTA controls the sampling frequency, it can control and demodulate applied jitter signals for seamless jitter transfer measurements as well as for analysis of any applied jitter signal, e.g., square-wave, triangle-wave, or random.

To appreciate the MTA technique, Figure 12, consider the sampler. The sampler is used as a mixer for frequency conversion. The signal at the sampler's output is the product of the input signal and the internally synthesized trigger signal. In an ideal sampler the input port briefly connects to the output port at a periodic rate. When connected, the output signal is the same as the input signal,

Figure 12. Block diagram of the Microwave Transition Analyzer.

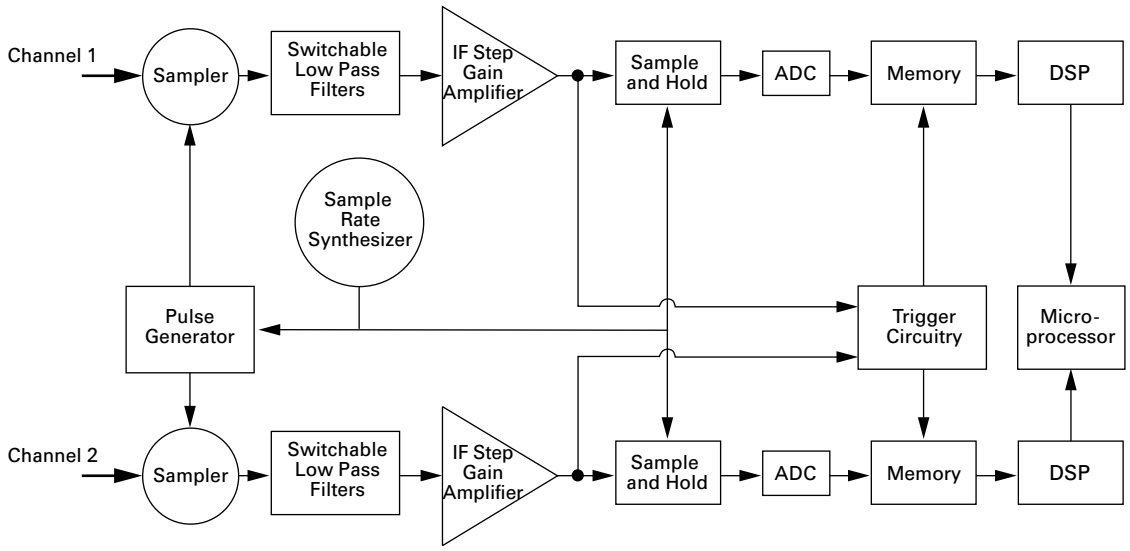

when not connected, it's zero. The synthesized trigger is a periodic pulse defining the connection as a function of time. The periodic pulse is therefore a frequency comb whose magnitude and phase is modulated by $\sin(2\pi fT)/2\pi fT$— the frequency spectrum of a rectangular shaped pulse. The result is that the frequency spectrum of the input signal is convolved with the spectrum of the periodic pulse to produce the spectrum at the sampler's output Intermediate Frequency (IF) signal. Deviations from the rectangular pulse shape, and hence the convolution and output, are corrected in the MTA Digital Signal Processor (DSP). The output of the ADC provides the demodulated jitter signal which is easily analyzed in either the time or frequency domains by using standard fast Fourier transforms.

The combination of a synthesized sampling frequency and a DSP make the MTA an excellent tool for demodulating and analyzing jitter, though, like any other technique based on signal sampling, low rate transient phenomena can escape detection.

3.2.3 The 71501D jitter analysis system

Figure 13 is a block diagram of the 71501D set-up for SONet/SDH/OTN jitter analysis. The 71501D jitter source, clock, and pattern generator can be included in Figure 7 (pg. 7) as discussed in Section 2.3.2 (pg. 7) for the 10 Gigabit Ethernet stressed eye receiver test. This is the same basic configuration as shown in Figure 5 (pg. 5) with the addition of the Modulation Test Set. The modulation test set does two things: it extends the applied jitter frequency and removes common-mode jitter from the clock source to lower the noise floor. Hardware filters for the standard SONet/SDH rates—155, 622, 2488, and 9953 Mb/s—are supplied with the 71501D; to ensure complete frequency agility, a template for implementation of a filter at any desired rate is also included. Jitter analysis by the MTA requires filtering, not just to set the spectrum for jitter generation, but to remove harmonics that can degrade the post processing and subsequent transfer accuracy.

To measure jitter generation, a non-jittered data pattern is used to stimulate the DUT. The DUT's recovered clock is sampled by the MTA. Displayed traces of the demodulated jitter signal and the reference clock in the time and frequency domains are useful debugging tools in high jitter environments. The rms level of the demodulated jitter signal yields the rms jitter generation measurement, J_{rms}, and the peak-to-peak extremes of the signal yield the peak-to-peak jitter, J_{PP}.

To measure jitter transfer a pattern generator is necessary and to measure jitter tolerance the complete BERT such as the 86130A or 71612C, including the analyzer (or error detector) is necessary. For jitter transfer, the two input channels, Figure 12 (pg. 13), are simultaneously (within 10 ps) sampled to accurately measure the ratio of the jitter amplitude received from the DUT to the amplitude applied to the data, $X_{Tfer}(f_J) = A_{out}(f_J) / A_{Appl}(f_J)$, over a narrow bandwidth centered on the applied jitter frequency. The frequency range and interval as well as custom specifications can be set by the user. The 71501D can also measure

Figure 13. Test setup for jitter analysis with the 71501D. This setup includes a complete BERT (i.e., a pattern generator complete with an error detector, e.g., Agilent 71612C) for SONet/SDH testing.

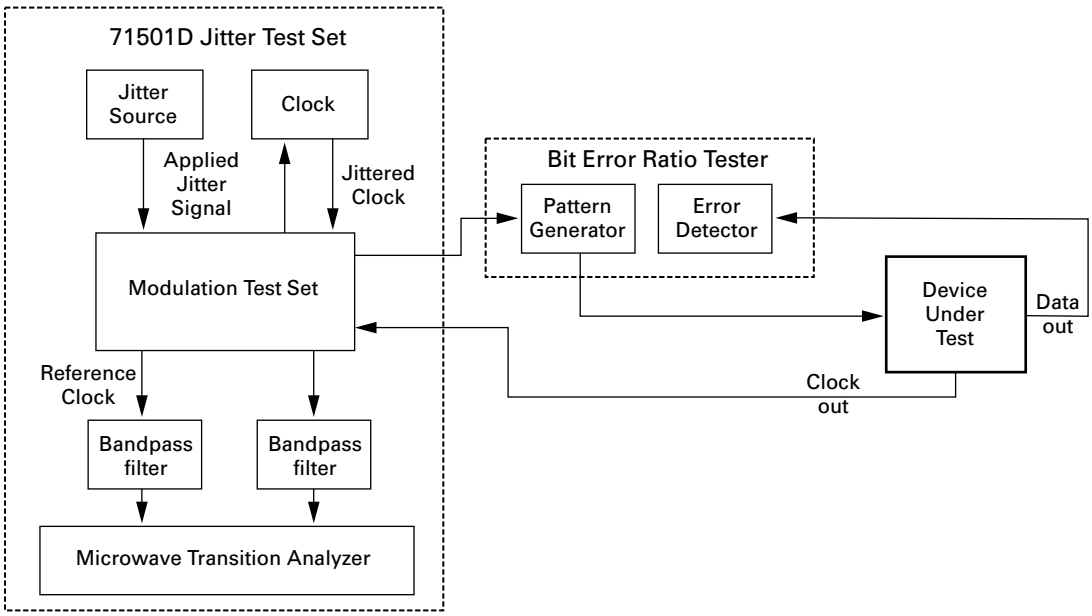

jitter transfer through a device where the input and output rates are not the same, which is useful for testing multiplexers and demultiplexers.

To measure jitter tolerance the DUT reconstructed clock provides timing for the BERT error detector and the DUT signal is analyzed by the error detector. In addition to testing compliance to the SONet/SDH/OTN specifications, the user can set a BER level to determine pass or fail status. A margin test can be performed by selecting a percentage margin by which to increase the jitter magnitude at each test point. A tolerance search is also available. In this mode the 71501D initially performs the BER test with jitter level set to that of a template. The jitter is then increased by a user-defined factor and a BER test is performed until either the desired BER limit or the test system generation capability is exceeded. The search factor can be set to either positive or negative levels so that $A_{Appl}(f_J)$ can be measured for almost any BER.

3.2.4 Summary of 71501D specifications

The 71501D automatically measures jitter generation, transfer and tolerance to the SONet/SDH/OTN standards. The 71501D can measure jitter on data rates ranging from 50 Mb/s to 12.5 Gb/s with applied jitter from 10 Hz to 80 MHz. The rms and peak-to-peak jitter noise floors are 2 and 20 mUI respectively. Jitter generation is measured with ±10% repeatability.

The 71501D includes the standard templates for SONet/SDH transfer and tolerance compliance tests, as well as customizable templates. DUTs can be stimulated with sinusoidal, square wave, triangle wave, and random applied jitter signals. Jitter can be applied with peak amplitudes in different frequency ranges[10]. The uncertainty of jitter transfer measurements vary with applied jitter frequency:

- ±0.05 dB from 10 Hz to 500 kHz,
- ±0.01dB from 500 kHz to 4 MHz, and
- ±0.02 dB from 4 MHz to 80 MHz.

When integrated into the 10 Gigabit Ethernet compliant stressed eye receiver test system, the 71501D delivers a calibrated level of jitter to the DUT.

3.3 Phase sensitive detection at fixed data rates—the OmniBER

3.3.1 Application focus

OmniBER is a family of SONet/SDH/OTN analyzers. Different models provide different SONet/SDH, Optical Transmission Network (OTN), Asynchronous Transfer Mode (ATM), and Packet Over SONet (POS) test suites at different sets of rates. They are primarily SONet/SDH/OTN functional and data-link layer test sets covering standard data rates from 1.5 Mb/s through 10.71 Gb/s with built in optical transmitters and receivers. Some of their capabilities include: the generation of structured SONet/SDH/ OTN framed data, event triggers for any transmitter or receiver alarm or error; the monitoring of all STS/AU signals, errors and alarm generations; frame capture, overhead sequence generation and capture, and a suite of Automatic Protection Switching (APS) tests including service disruption and active APS testing. Physical layer tests include BER tests, measurement of received optical power, deviation of the data rate from nominal rates, and as an optional feature, the test of jitter beyond SONet/SDH/OTN compliance levels. Jitter testing is the only feature of OmniBER that is addressed in this document.

OmniBER automatically measures jitter generation, jitter tolerance, jitter transfer, and, with available software, wander. It is restricted to standard SONet/SDH/OTN and E1/E2/E3/E4/DS1/DS3 clock rates–it is not frequency agile. OmniBER incorporates a specifically designed internal Clock Recovery (CR) circuit, as described in Section 2.5 (pg. 9), to measure jitter on data-only signals.

3.3.2 Jitter analysis with a phase detector

The OmniBER uses a phase detector to measure jitter from either the DUT's recovered clock output or its data output if a recovered clock isn't available from the DUT, as shown in Figure 14. Either the DUT clock output or the clock recovered by the OmniBER's CR from the DUT data output are mixed together. The data signal and the reference clock are maintained in quadrature by a Phase Locked Loop (PLL) circuit. The output of the mixer is subject to a bandpass filter that provides the SONet/SDH/OTN specified filter and rejects the high frequency content from the mixer to yield the demodulated jitter signal, $\varphi(t)$, in the jitter bandwidth of interest. The OmniBER analyzes the jitter signal to extract the standard jitter measurements. The OmniBER also provides the demodulated voltage output for external analysis on an oscilloscope, Digital Communications Analyzer, or spectrum analyzer—a useful diagnostic tool for debugging DUTs with large jitter.

The OmniBER CR circuit easily meets the requirements for passing the jitter of a data signal described in Section 2.5 (pg. 9): it synchronizes an internal clock to data transitions and has jitter generation well below the SONet/SDH/OTN specifications to be measured, a wide bandwidth, and a flat transfer function across the bandwidth of interest, to pass the jitter from the data through to the phase detector.

Jitter generation is measured by monitoring the demodulated jitter signals in real time to obtain J_{rms} and J_{PP} without distinguishing RJ and DJ. The peak-to-peak jitter is monitored over user defined measurement periods and continuously updates the results after each period.

For transfer and tolerance testing, the OmniBER uses an internal synthesizer to generate and impose sinusoidal jitter of defined amplitude and frequency, based on the SONet/SDH/OTN specifications, on the clock source that governs the pattern generator. An external input is also available for jitter injection. The data pattern can be framed SONet/SDH/OTN data or an unframed Pseudo Random Binary Sequence (PRBS). Since the OmniBER includes a complete BERT and separate reference and jittered clock sources, jitter tolerance is easily tested. Jitter tolerance and transfer can be displayed graphically and run automatically with the appropriate SONet/SDH/OTN mask.

Figure 14. The OmniBER's jitter analysis system uses a phase detector.

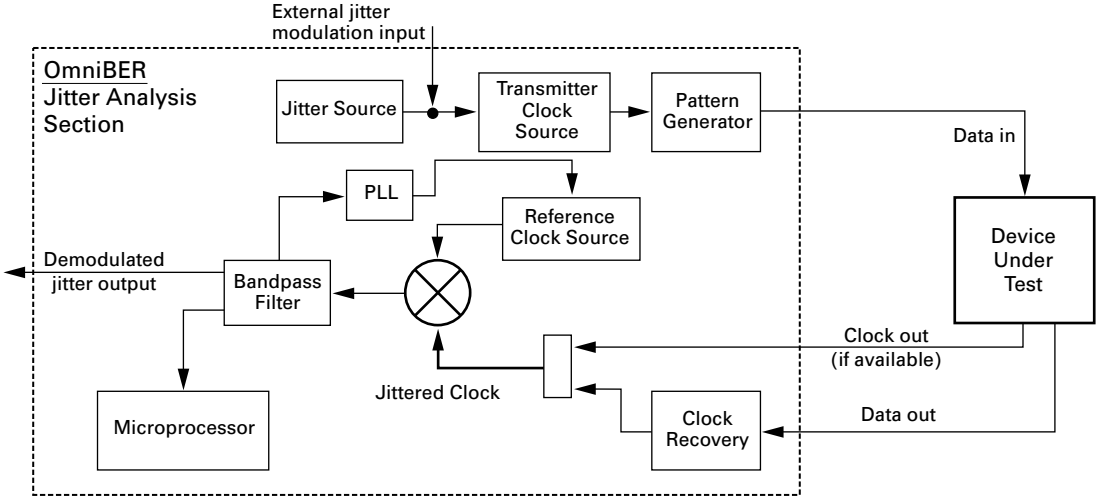

3.3.3 Summary of OmniBER jitter analysis specifications

OmniBER 2.5 Gb/s products (the 718, 719, and 725 models) automatically and exhaustively measure jitter to SONet/SDH specifications at standard fixed data rates from 1.5 Mb/s to 2.5 Gb/s. Two separate options are available with different noise floors including the CR circuit: Option 200 has a noise floor of no more than 50 mUI, and Option 210 of 35 mUI.

OmniBER OTN automatically and exhaustively makes measurements to SONet/SDH/OTN specifications at standard fixed data rates from 52 Mb/s to 10.71 Gb/s. Its noise floor is below 70 mUI with built in CR circuit. The user has full control over transfer and tolerance masks including detailed margin testing. A unique feature of the OmniBer OTN is that it can simultaneously measure jitter generation in a set of five different frequency bands enabling quick identification of specific jitter problems.

The jitter measurement noise floor and repeatability for peak-to-peak and rms jitter generation measurements, and the jitter transfer accuracy are given in Table 2.

3.4 Sampling oscilloscope analysis of jitter—the 86100 Infiniium digital communications analyzer

3.4.1 Application focus

The Infiniium Digital Communications Analyzer (DCA) is a high speed sampling oscilloscope that can perform a wide variety of pulse shape and eye-diagram measurements including peak-to-peak, J_{PP}, and rms, J_{rms}, jitter generation. The Infiniium DCA does not measure jitter tolerance or jitter transfer. Nor does it currently include software for separating Deterministic Jitter (DJ) and Random Jitter (RJ), however, the data set accumulated by the DCA can be downloaded to a PC where DJ and RJ can be separated offline as discussed in Section 3.4.4 (pg. 19). The data set so analyzed contains the same essential information available from a high-speed sampling Time Interval Analyzer (TIA).

Table 2. OmniBER jitter noise floor, repeatability, and transfer accuracy.

Bit Rate (Gb/s)	Jitter Amplitude Range (UI)	Noise Floor UI p-p	Noise Floor UI rms	Jitter Frequency Range (MHz)	Repeatability	Receiver Jitter (UI)	Jitter Transfer Accuracy (dB)
0.622	< 1.6	0.05	0.004	0.001 – 0.3	± 2%	> 0.3	0.04
	1.6 – 16	0.07	0.015	0.3 – 1	± 3%	0.3 – 0.1	0.15
	16 – 256	8	1.6	1 – 3	± 5%	0.1 – 0.03	0.25
				3 – 5	± 10%	0.03 – 0.01	0.5
2.488	< 1.6	0.05	0.004	0.005 – 0.3	± 2%	0.01 – 0.003	1
	1.6 – 64	0.1	0.03	0.3 – 1	± 3%	0.003 – 0.001	3
	64 – 1024	24	8	1 – 3	± 5%		
				3 – 10	± 10%		
				10 – 20	± 15%		
9.95/10.7		< 0.070	<< 0.070	0.02 – 0.3	± 2%		
				0.3 – 1	± 3%		
				3 – 10	± 10%		
				10 – 80	± 15%		

3.4.2 Sampling oscilloscopes

To achieve high bandwidth, the DCA samples the signal. The eye-diagram displayed does not represent complete individual overlapped logic pulses as on a real time oscilloscope. On a sampling oscilloscope, the eye is composed of data accumulated over many different pulses with no more than a single data point coming from a given pulse. For a sequential sampling oscilloscope, like the Infiniium DCA, a 'trace' of data is sequentially acquired at times, t_n, following each trigger pulse with

$$T_n = \frac{T_{FS}}{N-n}, \quad \text{for } n = 0, 1, 2, \ldots, N-1,$$

where T_{FS} is the scope's full screen 'sweep' time and N is the number of points across the horizontal width of the screen. After N data are acquired the process is repeated. Therefore, a clock signal is necessary to trigger data acquisition.

Accurate measurements of jitter on the DCA depend strongly on the quality of the trigger signal and the intrinsic jitter of the timebase. Any jitter in the trigger signal or timebase convolves with the jitter generation of the DUT contributing to the systematic error of the measurement. The trigger source can be the original clock from the signal transmitter or a clock recovered from the received signal.

The Agilent 8349x clock recovery devices use a phase locked loop (PLL) to synchronize an internal clock to data transitions. These devices include clocks at the standard SONet/SDH/OTN and Gigabit Ethernet rates. Since data transitions exhibit jitter, the bandwidth of the PLL used to synchronize the recovered clock to data transitions determines the level of jitter that passes through the recovered clock. The smaller the bandwidth, the less jitter that is passed into the recovered clock. The bandwidth of the PLL used by the 8349xA series of CDRs defaults to 50-70 kHz for jitter measurements. Notice that this application of CR circuits is different than the case in Section 2.5 (pg. 9) where wide bandwidth CRs are needed for measuring jitter generation and transfer on data-only signals with the JS-1000 or 71501. The difference is that the CR for the sampling oscilloscope provides a reference clock that must *not* pass the jitter to the sampling circuit because, here, the CDR provides a trigger relative to which jitter is observed. For the JS-1000 or 71501 the external CR must have a wide bandwidth to pass the jitter to the measurement system for comparison with a reference clock.

3.4.3 Measuring jitter generation with a sampling oscilloscope

The color grade data displayed on the DCA eye diagram is a two dimensional histogram, shown in Figure 15. Each pixel represents a given point in time and power, (t, P), (the vertical scale is power for optical signals and voltage for electrical). The color or intensity of a given pixel represents the number of data, N, acquired at that time, t, relative to the trigger pulse and power, P. Thus each point on the screen is a measurement of $N(t, P)$.

The Infiniium DCA measures jitter generation by projecting a pixel wide slice of the vertical axis onto the time axis, Figure 15. The resulting one dimensional histogram of time points is a statistical estimator of the probability distribution function of the signal's jitter generation. The standard deviation of the distribution is the rms jitter, J_{rms}. In the absence of DJ, the distribution should follow a Gaussian distribution and $J_{rms}^{RJ} = J_{rms}$. The peak-to-peak jitter generation, J_{PP}, is given by the distance in time between the two extreme data points.

Figure 15. Measurement of jitter generation on a sampling oscilloscope.

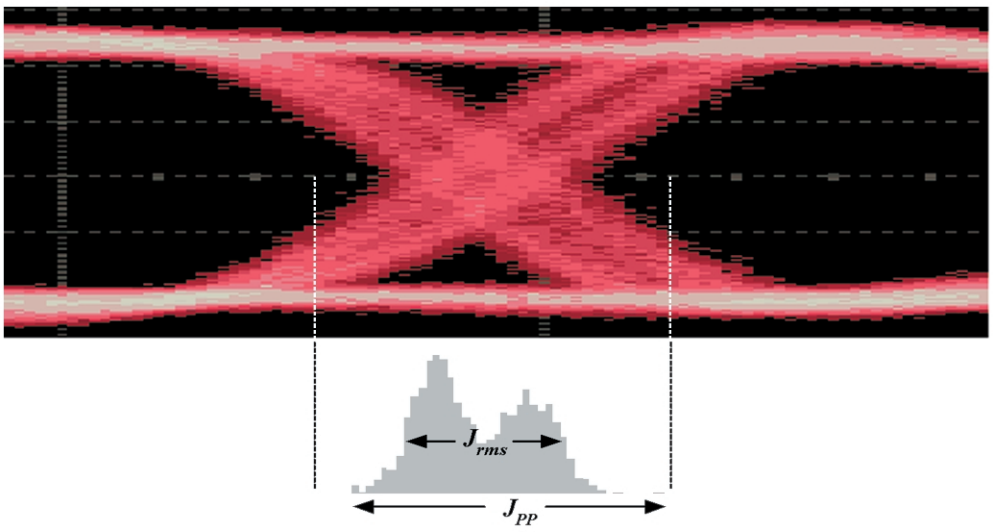

The SONet/SDH/OTN specifications require that jitter be measured only within certain bandwidths of jitter frequency for different data rates and wander is defined separately. Since the bandwidth of the DCA is considerably larger than the specified bandwidths, jitter generation measured by a DCA will be larger than the jitter generation measured by a SONet/SDH/OTN compliant test set, like the JS-1000, 71501D, or OmniBER.

3.4.4 Separating RJ and DJ using DCA data

DJ and RJ can be extracted from the DCA data set, $N(t, P)$: extract the time histogram at the crossing point, Figure 16b. Then fit[11] two separate Gaussian functions,

$$A\exp\left[-\frac{(t-\mu)^2}{2\sigma^2}\right],$$

to the edges. This technique is called a "scope scan" in Fibre Channel parlance. The fit yields the mean and width of the left and right Gaussians, (μ_L, σ_L) and (μ_R, σ_R) (A is the normalization). To obtain RJ, σ_L and σ_R are combined, by averaging them. Since DJ is bounded and RJ is distributed about these bounds, it is given by the difference of the means, Section 2.1.1 (pg. 2), $J^{DJ} = \mu_R - \mu_L$.

This data set has essentially the same information as a high-speed sampling TIA and faces the same problems. The primary issues are ambiguity, repeatability, and how to compare with other techniques, i.e., how to estimate the systematic error. The technique can be ambiguous because there are many different ways to perform the fit. Only the edges, where RJ is dominant, should be fit by a Gaussian, but one of the goals of the fit is to determine the transition point from the RJ dominated edge to the bounded DJ region. Three fitting techniques are commonly used.

First, a standard tail fitting approach: The edges of the distribution are numerically differentiated to determine the maxima, where $\partial N(t, P)/\partial t = 0$, and the points of inflection, where $\partial^2 N(t, P)/\partial t^2 = 0$, of the RJ distribution. The idea is to fit the tails while avoiding the DJ dominated interior region by including data in the fit from the tails up to some point between the inflection point and the

Figure 16. (a) The crossing point of the eye diagram from a Digital Communications Analyzer with a projection of the time histogram, $N(t, P)$. (b) Separating RJ and DJ by fitting Gaussian distributions to the histogram.

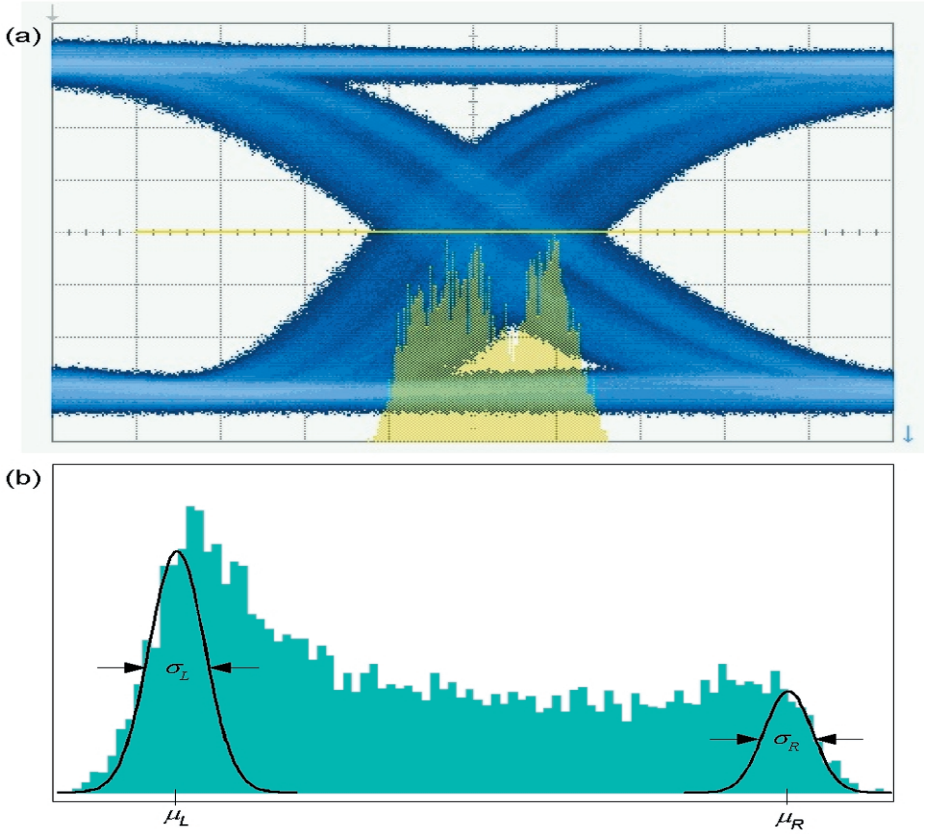

maximum. The data included in the fit is somewhat arbitrary and the results are difficult to reproduce because the derivatives are poorly defined. Derivatives calculated from empirical distributions vary with histogram binning; they change with random fluctuations in the distributions from different measurements of the same system; and, the end point of the data included in the fit between the inflection point and the maximum, while confined, is still arbitrary.

A less ambiguous approach is to parameterize the DJ dominated region and fit the whole distribution instead of just the tails. This is appealing because the parameterization of the DJ region can indicate different sources of DJ. The main problem is that there are already six free parameters in the fit with just the two Gaussians. The parameterization of DJ will contribute at least three more. A nine parameter fit on a distribution like that shown in Figure 16 (pg. 19) is not stable against random fluctuations and is therefore not likely to be reproducible.

A more stable approach is to perform several fits with just the two Gaussian tails. Each succeeding fit should include data closer to the DJ dominated region. When data is included from the DJ dominated region the confidence level rapidly increases. That fit with the largest confidence level yields the most accurate, repeatable parameters.

The repeatability problem with tail fitting is aggravated by the fact that fitting a Gaussian parameterization to a histogram is notoriously sensitive to isolated events in the tails (a.k.a., outliers) that cause the fit parameters, (μ_L, σ_L) and (μ_R, σ_R), to vary with different data samples. Outliers are a problem when the distribution is truly Gaussian, but experience from high rate SONet/SDH/OTN networks indicates that low BER DJ effects are often the most difficult to identify and remedy—this is the reason that peak-to-peak jitter measurements are pivotal in network design even though the true values are unbounded. If a DJ source has a BER less than, or around 10^{-4}, then the outliers are not contributed from random sources and the fit distribution does not actually follow a Gaussian. In this case, the tail fit is simply wrong.

Because of these issues, Agilent Technologies does not currently provide software for fitting the eye crossing point histogram. The bathtub plot method described in Section 3.5 is similar to fitting DCA data, but is usually less ambiguous and more repeatable[12].

3.5 Application of a bit error ratio tester—the "Bathtub Plot"

3.5.1 Application focus

Agilent offers several BERTs[13]: Agilent Technologies' 86130 BitAlyzer covers data rates from 0.050 to 3.6 Gb/s and Agilent Technologies' 71612C high speed BERT covers data rates from 0.100 to 12.5 Gb/s; and Agilent Technologies' 82150 family of Parallel Bit Error Ratio Testers, ParBERT, that cover data rates from 0.003 to 3.35 Gb/s, 9.5 to 10.8 Gb/s, and 38 to 45 Gb/s. They are all general purpose BERTs whose primary function is measuring the BER of data signals. They are also the key component in measuring transmitter dispersion penalty for 10 Gigabit Ethernet. None of them include protocol analysis, like the OmniBER, but they all offer many other unique features. The BitAlyzer has an excellent user interface and is equipped with powerful error analysis software that is a tremendous advantage in debugging hardware problems. The High-Speed BERT has four subrate outputs that are useful for testing multiplexed interfaces like the XAUI interface of 10 Gigabit Ethernet[14]. The modular ParBERT is extremely versatile and linearly scalable: separate data generators and analyzers can be configured together or independently. Because of its parallel nature, the ParBERT is ideal for testing mux/demux configurations and unique combinations of parallel-to-serial lines including the XAUI interface[15].

A BERT consists of a pattern generator, an error detector (or analyzer) and a system clock. The data generator generates a bit pattern, e.g., PRBS or formatted data frame or packet, that is transmitted to a DUT. The DUT then processes the bit pattern and transmits the result to the error detector. The error detector synchronizes on the known pattern, counts the number of received bits, determines which bits were received in error, and calculates the BER. The sampling point, shown in Figure 2 (pg. 2), is usually positioned at the center of the eye—if the received power is above the sampling point then the bit is identified as a logic "1", if below, a "0". Jitter can be measured on a BERT by stepping the sampling point across the eye into the eye crossing region. The BER increases due to the effect of jitter as the sampling point approaches the crossing point.

3.5.2 Measuring Jitter with a BERT

To analyze jitter generation, the BER is measured as a function of the sampling point's time position. In Fibre Channel parlance, this process is called a "BERT scan." The graph of BER vs t, Figure 17, is called a "bathtub plot" (a functionally equivalent analysis can be performed by studying BER(t) from one end of the crossing point to the other, these are called "Rastafarian plots"). As the sampling point is stepped from the center toward the eye crossing, the BER increases continuously until reaching a maximum of 0.5 (if there are an equal number of "1"s and "0"s in the pattern, i.e., equal transition density). The structure of the bathtub plot reflects RJ and different types of DJ.

Let the left edge of the relative time position of the eye diagram be $t = 0$ and the right be $t = T_b$, the bit period. As the sampling point moves from the center, $\frac{1}{2}T_b$, toward an edge, it begins in the region where the BER is dominated by RJ. In the regions $t \le T_L^{DJ}$ on the left side, or $t \ge T_R^{DJ}$ on the right side, the BER is dominated by DJ. These points, T_L^{DJ} and T_R^{DJ}, are related to the peak-to-peak DJ by $J_{PP}^{DJ} = T_L^{DJ} + (T_B - T_R^{DJ})$, Figure 4 (pg. 3). In the DJ dominated region $\mathrm{BER}_{DJ}(t)$ can be described with different functional forms for different types of jitter. For example, sinusoidal jitter of amplitude A is described by $\mathrm{BER}_{sinusoidal}(t) = \frac{1}{2} - 1/\pi \arcsin(t/A)$ and intersymbol interference (ISI) can result in plateaus in the eye diagram. The functional forms of the left and right regions of DJ should be the same, but with different symmetry, since the underlying causes of jitter are not unique to a given edge. To summarize:

$$\mathrm{BER}(t) = \begin{cases} \mathrm{BER}_{DJ}^{L}(t), & 0 < t < T_L^{DJ} \\ \mathrm{BER}_{RJ}(t), & T_L^{DJ} < t < T_R^{DJ} \\ \mathrm{BER}_{DJ}^{R}(t), & T_R^{DJ} < t < T_B \end{cases} \tag{6}$$

The effect of RJ is to form smooth continuous curves rising to higher BERs as the sampling point approaches either eye edge. This behavior reflects the Gaussian nature of RJ and can be expressed with the complementary error function, as derived in Appendix B (pg. 25), for the left edge,

$$\begin{aligned} \mathrm{BER}_{RJ}^{L}(t) &= \frac{1}{\sigma_L}\sqrt{\frac{2}{\pi}} N_L \int_t^{\infty} \exp\left[-\frac{(t' - T_L^{DJ})^2}{2\sigma_L^2}\right] dt' \\ &= N_L \mathrm{erfc}\left(\frac{t' - T_L^{DJ}}{\sqrt{2}\sigma_L}\right) \end{aligned} \tag{7}$$

where N_L is determined by continuity of BER(t) at T_L^{DJ} and T_R^{DJ}. Notice that the mean of the Gaussian distribution is T_L^{DJ}, and as expected from the discussion in Section 2.1 (pg. 3), joins continuously with the onset of DJ. Equation (7), the continuity conditions, and the expression for the right side are derived in Appendix B (pg. 25).

RJ and DJ can be separated by fitting[11] the sum of RJ contributions from the left and right edges,

$$\mathrm{BER}_{RJ}(t) = N_L \mathrm{erfc}\left(\frac{t' - T_L^{DJ}}{\sqrt{2}\sigma_L}\right) + N_L \mathrm{erfc}\left(\frac{T_R^{DJ} - t}{\sqrt{2}\sigma_R}\right), \tag{8}$$

to the tails of the BER(t) distribution with six free parameters: (T_L^{DJ}, σ_R, N_L) and (T_R^{DJ}, σ_L, N_R). The normalization constants, N_L and N_R, are the BER at the RJ-DJ transition points, $t = T_L^{DJ}$ and $t = T_R^{DJ}$ and are derived for the general case of any DJ level or shape, in Appendix B (pg. 25). In

Figure 17. A bathtub plot, BER vs. *t*, illustrating the regions dominated by RJ and DJ.

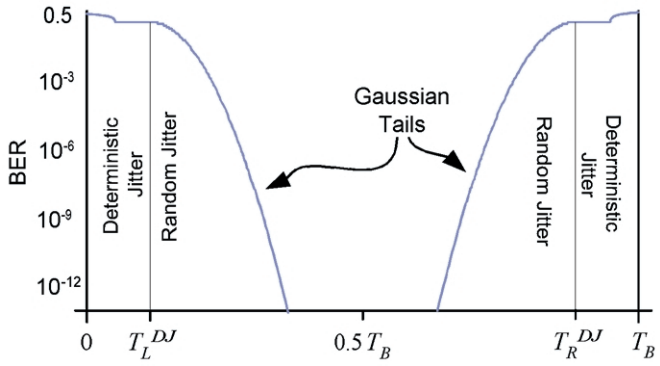

practice, approximations are usually made to Eq. (8) (pg. 22) to speed up the computation. First, since the measurement is usually performed on reasonably clean eyes, the contribution of the Gaussian tail from the right edge of the eye is neglected in fitting the left edge reducing to Eq. (7) (pg. 22). Second, Eq. (7) is inverted by using an approximation to the inverse of the error function,

$$\text{erf}^{-1}(x) \cong 1.192 - 0.6681 \log(x) - 0.0162 \left(\log(x)\right)^2 \quad (9)$$

to yield an equation linear in t of the form $y = A_0 + A_1 t$ which can be fit to the data using the least squares technique. The fit parameters A_0 and A_1, along with Eq. (9) are used to convert back to Eq. (7)—the details are given in Appendix C (pg. 27)—from which the key parameters, σ_L, σ_R, T_L^{DJ}, and T_R^{DJ}, are extracted to yield

$$J_{rms}^{RJ} = \tfrac{1}{2}(\sigma_L + \sigma_R) \quad \text{and} \quad J_{PP}^{DJ} = T_L^{DJ} + (T_B - T_R^{DJ}).$$

The jitter margin at a given BER is then easily calculated; e.g., for BER = 10^{-12} using Table 1 and Eq. (1) (pg. 5), the total peak-to-peak jitter is given by $J^{TJ} = 14.1 \times J_{rms}^{RJ} + J_{PP}^{DJ}$. Alternatively, with the fitted curves included in Figure 17 (pg. 21) J^{TJ} can be read off the bathtub plot for a given BER.

While the cause is not well understood, σ_R and σ_L are not equal. In fact, the difference between the two is more pronounced in optical than electrical systems. Note also that, in general, the level of DJ at $t = T_R^{DJ}$ is not the same as the level at $t = T_L^{DJ}$ because of differences in the rising and falling edges of logic pulses.

This technique measures RJ and DJ jitter generation relatively quickly and with minimal loss of accuracy, the fit parameterizations can be extrapolated to the BER of interest. For example, at 10 Gb/s, it would take nearly an hour to measure the BER(t) distribution including points at BER = 10^{-12}, but if the fit includes points out to BER = 10^{-9}, the results are available in about a minute. Alternatively, if a system is suspected to have low rate DJ, the measurement can be carried out to any BER without curve fitting. For this reason the BER(t) measurement is usually the standard by which other techniques are evaluated.

Fitting the BER(t) distribution to measure jitter and separate RJ and DJ is usually faster, less ambiguous, and more repeatable than fitting the crossing point histogram, discussed in Section 3.4.4 (pg. 19). It is faster because the data used in the fit is acquired at the full data rate. Sampling scopes acquire their data at a lower rate, and the single pixel wide region covering the eye crossing point is a small subset of the data. It is usually less ambiguous and more reliable for several reasons: First, the BER(t) distribution is unambiguously binned by the BER measurement; second, since it is simple to require a minimum number of errors in each BER measurement, there are no problems with isolated random events in the tails of the RJ distribution; third, if the DJ dominated region is included in the fit, a priori parameterizations for different sources of DJ can be included—though, as the number of fit parameters increases the stability of the fit decreases here too; fourth, the normalization parameters in the fit, Eq. (8) and Eq. (11), depend on the other fit parameters and can be used to check consistency.

A systematic problem that should be addressed in fitting the BER(t) distribution is the effect of the vertical position of the crossing points with respect to the vertical position of the sampling point. If the crossing points are not at the same power level as the sampling point, then as the sampling point is stepped toward an edge, it will encounter the rising/falling edges of the bits, Figure 2 (pg. 2). If the sampling point is stepped into a rising or falling edge instead of the crossing point, the BER(t) increases prematurely and biases the value of DJ above its true value. However, the bias may be appropriate because live data is converted to logic values just as it is in a BERT, but purely in terms of jitter, results from a fit of BER(t) in this environment are difficult to compare with results from the more direct techniques like phase analysis.

Agilent Technologies provides software with each BERT to measure and fit the BER(t) distribution that allows the user to choose the data accumulation parameters such as how many data points to acquire on each edge, the time spacing between them, and the minimum number of errors required at each point[16].

4. Comparison of the techniques

Measurement of jitter in high rate network elements is necessary at all stages of product development: in the research lab, to test the utility of new technologies; in development, for improving performance and compliance testing; and in manufacturing, installation and maintenance, for quality control as well as system specification testing. The five different techniques and systems for jitter characterization are summarized in Table 3.

Comparison of well defined band-limited measurements, such as SONet/SDH/OTN compliance testing on the JS-1000, 71501D, or OmniBER are straightforward as long as the uncertainty and repeatability of the measurements are considered. But it can be difficult to compare jitter measurements from very different techniques. A common source of confusion results from comparing band-limited jitter generation J_{PP} and J_{rms} measurements on an OmniBER with a wide bandwidth measurement on a DCA. A more complicated example is the comparison of DJ components identified in the phase noise plot produced by the JS-1000 with peak-to-peak DJ, J_{PP}^{DJ}, measured by fitting the tails of the bathtub plot from a BERT. This comparison is complicated by the fact that in addition to the band-limited nature of measurements with the JS-1000, the discrete DJ components may not sum to the total DJ of the system without a careful model of the phase noise plot. An example of two measurements that should, but might not, be comparable is the separation of RJ and DJ by fitting the bathtub plot and by tail fitting the histogram from a sampling oscilloscope (DCA) or sampling TIA. The comparison is complicated by the fundamental ambiguity of the tail-fitting method and the possibility that the histogram may not have been extracted at the same power level at which the sampling point was set as it was scanned across the eye to measure the bathtub plot. This is an example where the histogram extracted from a DCA is easier to interpret than the histogram from a TIA.

To summarize, in comparing jitter measurements performed with very different techniques it is useful to (1) keep in mind the jitter frequency band limiting nature of the techniques; (2) make comparisons that allow for uncertainty from the combination of noise floor and repeatability of the measurements; and (3) to understand the systematic differences of the techniques.

Table 3. A summary comparing the five jitter analysis techniques reviewed in this note—for complete specifications, please use the Technical Specifications documents available at www.agilent.com/find/jitter.

	JS-1000	71501D	OmniBER	Infiniium DCA	Bit Error Ratio Testers
Highest Data Rate	45 Gb/s	12.5 Gb/s	10.71 Gb/s	> 40 Gb/s	45 Gb/s
Fixed or agile data rates	Agile	Agile	Fixed	Agile	Agile
Real-time or sampling	Real-time	Sampling	Real-time	Sampling	N/A
Typical rms noise floor (for low jitter amplitudes)	< 50 μUI	2 mUI	4 mUI[1]	0.85 ps 200 fs[2]	N/A
Typical rms repeatability (for low jitter amplitudes)	± 5%	± 10%	< ± 20%	N/A	N/A
Typical PP noise floor		20 mUI	50 mUI	4.0 ps 800 fs[2]	N/A
Typical jitter transfer accuracy (at 1 MHz)	± 0.01 dB	± 0.01 dB	± 0.04 dB	N/A	N/A
Measure on data-only signals	Optional CR required[3]	External CR required[3]	✓	✓	✓
Automatically separate RJ and DJ					✓
Identify DJ signals[4]	✓				
Built-in optical interface[5]			✓	✓	
SONet/SDH/OTN compliant	✓	✓	✓		
Measures wander independent of jitter to SONet/SDH specifications			✓[6]		
Part of the transmitter dispersion penalty test set (for 10 Gigabit Ethernet)					✓
Part of a stressed eye receiver sensitivity test set (for 10 Gigabit Ethernet)	✓	✓		✓	✓
SONet/SDH/OTN functional and Data-link-layer test			✓		

1. Including the effect of the built in clock recovery circuit for jitter on data only signals.
2. Using the 86107A precision time base.
3. Use of an external Clock Recovery (CR) circuit substantially raises the noise floor.
4. The 71501D and OmniBER both provide the demodulated jitter signals that can be used to identify DJ sources, but the JS-1000 has a much lower noise floor and automatically identifies spurs in the phase-noise plot.
5. For measurements on optical signals by those systems that do not have them built in, Agilent Technologies makes a variety of appropriate optical transmitters and receivers.
6. With optional software.

Appendices

Appendix A: The relationship between single side band phase noise and phase deviation spectral density

The Single-Side-Band (SSB) phase noise, $\mathcal{L}(f)$, can be related to the phase deviation spectral density. Consider the signal in a phasor diagram with phase noise and amplitude noise, as shown in Figure 18. Amplitude noise sweeps a circle of radius ΔV_{noise} centered at the tip of the signal vector. The uncertainty in the phase, i.e., the phase noise, is given by $\tan(\Delta\varphi(t)) = \Delta V_{noise}/V_{carrier}$.

Using the small angle approximation gives $\Delta\varphi(t) = \Delta V_{noise}/V_{carrier}$. The SSB power density with respect to the carrier is

$$\mathcal{L}(f) = \frac{1}{\Delta f}\,\frac{\frac{1}{2}\Delta V^2_{Noise\ rms}/R}{V^2_{Carrier}/R} = \frac{1}{2\Delta f}\,\frac{\Delta V^2_{Noise\ rms}}{V^2_{Carrier}}$$

$$= \frac{\Delta\varphi^2_{rms}}{2\Delta f}$$

$$= \tfrac{1}{2} S_\varphi(f)$$

Since 'radians' are not dimensions in the same sense as volts or watts, there's no inconsistency in relating the dimensions of $\mathcal{L}(f)$ and $S_\varphi(f)$, to give Eq. (3):

$$\mathcal{L}(f)\left[{}^{1}/_{\mathrm{Hz}}\right] = \tfrac{1}{2} S_\varphi(f)\left[{}^{\mathrm{rad}^2}/_{\mathrm{Hz}}\right]$$

If the SSB spectrum is measured by a spectrum analyzer, amplitude noise distorts the spectrum from the ideal, $\mathcal{L}(f) = \tfrac{1}{2} S_\varphi(f)$. The component of ΔV_{noise} in phase with (parallel to) the carrier vector, $V_{carrier}$, appears as noise in the frequency spectrum because the amplitude noise, ΔV_{noise}, varies with time. But this noise is amplitude noise not, phase noise. Only those variations in the component of ΔV_{noise} perpendicular to the carrier cause deviations in the phase, $\Delta\varphi(t)$. The advantage of a phase detector system measuring $S_\varphi(f)$ is that only the phase deviations are measured, giving a lower noise floor.

Figure 18. The relationship between phase noise and amplitude noise.

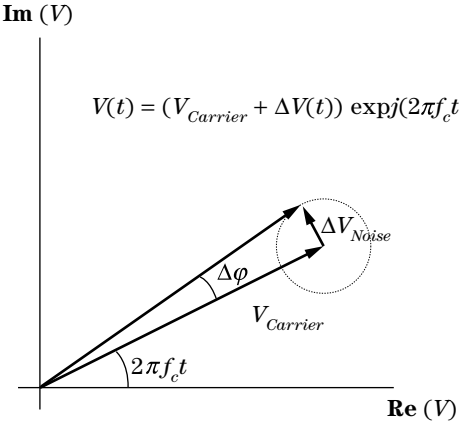

Appendix B: The relationship between jitter and bit error ratio

In this appendix an expression for the BER as a function of the time position of the sampling point in the central region of the eye, where horizontal eye closure is due to RJ, $T_R^{DJ} < t < T_L^{DJ}$, is derived for the general case applicable to any type of DJ. We make three assumptions: first, that the data has 50% transition density; second, that RJ follows a Gaussian distribution; and third, that the vertical position of the sampling point is accurately tuned to approach the mean crossing point of the eye.

First, only consider the effect of the RJ from the left crossing point of the eye, this will give us Eq. (7) of Section 3.5.2 (pg. 22). Then we generalize for the right side and add the two terms together to get Eq. (8). As shown in Figure 2 (pg. 2) the left eye crossing point is chosen at $t = 0$. The Gaussian nature of RJ means that the probability of the edge of a given bit being in the range t' to $t' + dt$ is given by the probability density function

$$\rho(t')\,dt = \frac{1}{\sigma_L}\sqrt{\frac{2}{\pi}}\,N_L \exp\left[-\frac{(t' - T_L^{DJ})^2}{2\sigma_L^2}\right]dt$$

This is a Gaussian distribution centered at the onset of DJ, T_L^{DJ}, with width, or standard deviation, $\sigma = J_{RMS}^{RJ}$. The normalization, N, is determined by the effect of DJ on the BER at the extreme edges of the J_{PP}^{DJ} distribution, as shown below. The probability of a given bit being misidentified is the probability that the edge of the bit is on the wrong side of the sampling point. Concentrating on just the left side of the eye, this is the total probability that the edge is to the right of the sampling position, t:

$$\mathrm{BER}_{RJ}^{L}(t) = \frac{1}{\sigma_L}\sqrt{\frac{2}{\pi}}\,N_L \int_t^\infty \exp\left[-\frac{(t' - T_L^{DJ})^2}{2\sigma_L^2}\right]dt' \qquad (10)$$

To convert this to standard form, let $u = (t - T_L^{DJ}) / (\sqrt{2}\,\sigma)$, then Eq. (9) becomes

$$\mathrm{BER}_{RJ}^{L}(t) = \frac{2}{\sqrt{\pi}} N_L \int_{\frac{t - T_L^{DJ}}{\sqrt{2}\,\sigma_L}}^{\infty} e^{-u^2} du$$

Recall that the error function and complementary error function are given by

$$\mathrm{erf}(t) = \frac{2}{\sqrt{\pi}} \int_0^t e^{-u^2} du \quad \text{and}$$

$$\mathrm{erfc}(t) = 1 - \mathrm{erf}(t) = \frac{2}{\sqrt{\pi}} \int_t^{\infty} e^{-u^2} du.$$

Equation (10) can then be expressed as

$$\mathrm{BER}_{RJ}^{L}(t) = N_L \,\mathrm{erfc}\left(\frac{t - T_L^{DJ}}{\sqrt{2}\sigma_L}\right).$$

Now consider the right side of the eye. Going through the same steps as for the left side, but using a slightly different substitution,

$$\mathrm{BER}_{RJ}^{R}(t) = N_R \,\mathrm{erfc}\left[\frac{T_R^{DJ} - t}{\sqrt{2}\sigma_R}\right].$$

The normalizations, N_L and N_R, are determined by requiring continuity of BER(t) in Eq. (6) at $t = T_L^{DJ}$ and $t = T_R^{DJ}$. The BER at these two points is determined by DJ. We get two equations

$$\mathrm{BER}_{RJ}^{L}(T_L^{DJ}) = N_L + N_R \,\mathrm{erfc}\left[\frac{T_R^{DJ} - T_L^{DJ}}{\sqrt{2}\sigma_R}\right] \text{ and}$$

$$\mathrm{BER}_{RJ}^{R}(T_R^{DJ}) = N_L \,\mathrm{erfc}\left[\frac{T_R^{DJ} - T_L^{DJ}}{\sqrt{2}\sigma_L}\right] + N_R$$

Let $\xi_{L/R} = \mathrm{erfc}[(T_R^{DJ} - T_L^{DJ}) / (\sqrt{2}\,\sigma_{L/R})]$ and solve for N_L and N_R:

$$N_L = \frac{\mathrm{BER}_{DJ}^{L}(T_L^{DJ}) - \xi_R \,\mathrm{BER}_{DJ}^{R}(T_R^{DJ})}{1 - \xi_R \xi_L}$$

$$N_R = \frac{\mathrm{BER}_{DJ}^{R}(T_R^{DJ}) - \xi_L \mathrm{BER}_{DJ}^{L}(T_L^{DJ})}{1 - \xi_R \xi_L} \qquad (11)$$

The BER as a function of the time position of the sampling point in the central region of the eye, $T_R^{DJ} < t < T_L^{DJ}$, where horizontal eye closure is due to RJ is therefore given by

$$\mathrm{BER}_{RJ}(t) = \left(\frac{\mathrm{BER}_{DJ}^{L}(T_L^{DJ}) - \mathrm{erfc}\left[\frac{T_R^{DJ} - T_L^{DJ}}{\sqrt{2}\sigma_R}\right]\mathrm{BER}_{DJ}^{R}(T_L^{DJ})}{1 - \mathrm{erfc}\left[\frac{T_R^{DJ} - T_L^{DJ}}{\sqrt{2}\sigma_R}\right]\mathrm{erfc}\left[\frac{T_R^{DJ} - T_L^{DJ}}{\sqrt{2}\sigma_L}\right]}\right)\mathrm{erfc}\left(\frac{t - T_L^{DJ}}{\sqrt{2}\sigma_L}\right)$$

$$\left(\frac{\mathrm{BER}_{DJ}^{R}(T_R^{DJ}) - \mathrm{erfc}\left[\frac{T_R^{DJ} - T_L^{DJ}}{\sqrt{2}\sigma_L}\right]\mathrm{BER}_{DJ}^{L}(T_L^{DJ})}{1 - \mathrm{erfc}\left[\frac{T_R^{DJ} - T_L^{DJ}}{\sqrt{2}\sigma_R}\right]\mathrm{erfc}\left[\frac{T_R^{DJ} - T_L^{DJ}}{\sqrt{2}\sigma_L}\right]}\right)\mathrm{erfc}\left(\frac{T_R^{DJ} - t}{\sqrt{2}\sigma_R}\right)$$

Appendix C: Standard method for extraction of RJ and DJ from the bathtub plot, BER(t)

The standard approach to separating RJ and DJ by fitting Gaussian tails to the inner edges of the bathtub plot, BER(t), assumes that the BER from the left edge is independent of jitter from the right edge and vice versa. It is therefore sufficient to demonstrate the procedure for one side of the bathtub plot. Let the measured points be given by (r_i, t_i) where r_i is the measured BER for a sampling point centered at time t_i. To separate RJ and DJ we fit the tail of a Gaussian distribution,

$$\mathrm{BER}_{RJ}(t) = N\,\mathrm{erfc}\left(\frac{t - T^{DJ}}{\sqrt{2}\sigma}\right) \tag{12}$$

to this data set using linear regression. Equation (12) can be written

$$1 - \frac{\mathrm{BER}_{RJ}(t)}{N} = \mathrm{erfc}\left(\frac{t - T^{DJ}}{\sqrt{2}\sigma}\right)$$

Using the approximation for $\mathrm{erf}^{-1}(x)$ given in Eq. (9) and a bit of rearrangement

$$\sqrt{2}\,\mathrm{erf}^{-1}\left(1 - \frac{\mathrm{BER}_{RJ}(t)}{N}\right) = -\frac{T^{DJ}}{\sigma} + \frac{1}{\sigma}t \tag{13}$$

Which has the form $y = A_0 + A_1 t$ with $T^{DJ} = -A_0/A_1$ and $\sigma = 1/A_1$.

Linear regression is simply the process of minimizing the sum of the squares of the differences of the data points and the linear parameterization, Eq. (13). Let

$$y_i = \sqrt{2}\,\mathrm{erf}^{-1}\left(1 - \frac{r_i}{N}\right) \text{ and } \eta = \sum_i [y_i - (A_0 + A_1 t)]^2$$

η is similar to χ^2 but without the BER measurement uncertainty included. Linear regression consists of determining the minimum of η by solving the simultaneous equations $d\eta/dA_0 = 0$ and $d\eta/dA_1 = 0$. It is described in reference 6 (pg. 28). A simple way to assure that the fit reasonably follows the measurements is to require that the coefficient of determination (which is not to be confused with a confidence level) of y and t be larger than 0.95.

References

1. Agilent Technologies' E1725C and E1740A Time Interval Analyzers, have been discontinued. A more modern approach to jitter analysis for data rates below the Gb/s level that uses a similar technique is provided by the Agilent 53310A Modulation Domain Analyzer, details are available at **www.agilent.com/find/53310a.**

2. See Agilent Technologies Product Note, "Jitter Analysis Techniques Using an Agilent Infiniium Oscilloscope," literature number 5988-6109EN, 2002. Available from **www.agilent.com/find/jitter.**

3. The standards referenced in this document as "SONet/SDH specifications" are ITU-T 0.172, **www.itu.int**, and GR-253-CORE, **www.telcordia.com.**

4. The standards referenced as Gigabit Ethernet and 10 Gigabit Ethernet are IEEE 802.3z and 802.3ae and can be found at **standards.ieee.org/getieee802/**.

5. NIST Technical Note 1337, "Characterization of Clocks and Oscillators," edited by D.B. Sullivan, D.W. Allan, D.A. Howe, F.L. Walls, 1990.

6. See any standard probability and statistics text, for example, Anthony J. Hayter, *Probability and Statistics For Engineers and Scientists, 2nd ed.* (Brooks/Cole Publishing, 2002).

7. For a complete discussion of phase noise see, W. P. Robins, *Phase Noise in Signal Sources* (*Theory and Applications*), (Peter Peregrinus Ltd., 1982).

8. J.A. Barnes and D.W. Allan, "A Statistical Model of Flicker Noise," Proc. IEEE, Vol. 43, pp. 176-178, February 1966.

   An easily accessible reference is **www.boulder.nist.gov/timefreq/phase/Properties/twelve.htm.**

9. David J. Ballo and John A. Wendler, "The New Microwave Transition Analyzer: A New Instrument Architecture for Component and Signal Analysis," Hewlett-Packard Journal, October, 1992.

10. Agilent Technologies' 71501D Product Overview, "A Flexible Wide Bandwidth Jitter Analysis System," literature number 5988-5234EN. Available from **www.agilent.com/find/jitter.**

11. William H. Press et al, *Numerical Recipes in C: The Art of Scientific Computing, 2nd ed.* (Cambridge University Press, New York, 1997). This text has several examples of how to perform multi-parameter regressive fits.

12. See IEEE 802.3ae D5.0, May 2002, p. 357.

13. Technical specifications, data sheets, related product and application notes on all Agilent products are available from **www.agilent.com.**

14. Geoff Waters, Agilent Technologies' 71612C Product Note, "10 Gigabit Ethernet and the XAUI Interface," literature number 5988-5509EN, 2002. Available from **www.agilent.com/find/10ge.**

15. Agilent Technologies' 81250 ParBERT Application, "10 GbE Technology and Device Characterization," literature number 5988-6960EN, 2002. Available from **www.agilent.com/find/10ge.**

16. Agilent Technologies Bathtub Jitter Software runs on the 71612C and ships with the 86130A BitAlyzer and is available to download from the 86130A web page under: software, firmware, drivers **www.agilent.com/comms/bitalyzer.**

www.agilent.com

Agilent Email Updates

www.agilent.com/find/emailupdates
Get the latest information on the products and applications you select.

Agilent T&M Software and Connectivity
Agilent's Test and Measurement software and connectivity products, solutions and developer network allows you to take time out of connecting your instruments to your computer with tools based on PC standards, so you can focus on your tasks, not on your connections.
Visit **www.agilent.com/find/connectivity** for more information.

By internet, phone, or fax, get assistance with all your test & measurement needs

Online assistance:
www.agilent.com/find/assist

Phone or Fax

United States:
(tel) 800 452 4844

Canada:
(tel) 877 894 4414
(fax) (905) 282 6495

China:
(tel) 800 810 0189
(fax) 800 820 2816

Europe:
(tel) (31 20) 547 2323
(fax) (31 20) 547 2390

Japan:
(tel) (81) 426 56 7832
(fax) (81) 426 56 7840

Korea:
(tel) (82 2) 2004 5004
(fax) (82 2) 2004 5115

Latin America:
(tel) (305) 269 7500
(fax) (305) 269 7599

Taiwan:
(tel) 0800 047 866
(fax) 0800 286 331

Other Asia Pacific Countries:
(tel) (65) 6375 8100
(fax) (65) 6836 0252
(e-mail) tm_asia@agilent.com

Product specifications and descriptions in this document subject to change without notice.

Printed in USA. February 3, 2003
5988-8425EN

Agilent Technologies